Supporting Information

Cyclometalated (NNC)Ru(II) complex catalyzed β-methylation of alcohols using methanol

Kasturi Ganguli[a], Natalia V. Belkova[b] and Sabuj Kundu[a]*

[a]Department of Chemistry, Indian Institute of Technology Kanpur, Kanpur-208016, India

[b]A.N. Nesmeyanov Institute of Organoelement Compounds, Russian Academy of Sciences (INEOS RAS), Vavilova Str. 28, 119991 Moscow, Russia

*Email: sabuj@iitk.ac.in

Table of Contents

	Page
1. General procedure for time dependent experiment	**3**
2. Kinetic Isotope Effect (KIE) studies	**3-4**
3. Synthesis of Ru(II) hydride	**4-7**
3.1 Generation of Ru(II) hydride in presence of $LiHBEt_3$	**4-5**
3.2a In-situ generation of Ru(II)-hydride	**5-7**
3.2b Utilizing *in-situ* generated Ru(II)-hydride (B)′ for the β-methylation of 1-phenylpropanol:	**7**
3.2c In-situ detection of Ru(II)-methoxide intermediate	**7-8**
4. X-Ray crystallographic studies	**8-11**
5. Copies of ^{1}H and ^{13}C NMR Spectra	**12-41**

1. General procedure for time dependent experiment:

Several identical experiments for the β-methylation of 1-phenylethanol were performed in a parallel manner under the conditions for general procedure for the selective monomethylation of secondary alcohols with varying time (0 to 24 h). The progress of the reaction was monitored by gas chromatography using mesitylene as internal standard. All the reactions were repeated twice and the average data were plotted as yield (%) vs time (h) (Figure **S1**).

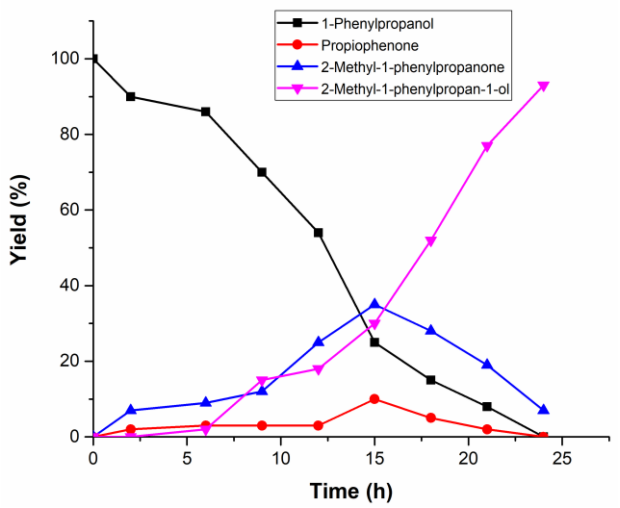

Figure S1. Time dependent product distribution during the formation of 2-methyl-1-phenylpropan-1-ol (**4**) from 1-phenylpropanol (**1**).

2. Kinetic Isotope Effect (KIE) studies

Parallel reactions for the synthesis of 2-methyl-1-phenylpropanol (**4**) from 1-phenylpropanol were carried out in both CH_3OH and CD_3OD following the outlined procedure (general procedure for the selective monomethylation of secondary alcohols). All the tubes were placed in a preheated oil-bath at 140 °C and heated for specified time. The progress of the reaction was analyzed by GC using mesitylene as internal standard. All the reactions were repeated thrice and the average conversion of **1** as ln(a/a-x) vs time (hour). The ratio of slope of the two plots directly gave the $k_{C\text{-}H}/k_{C\text{-}D}$ value (Figure **S2**).

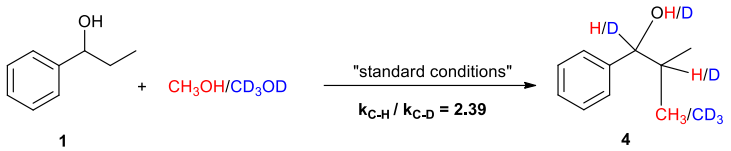

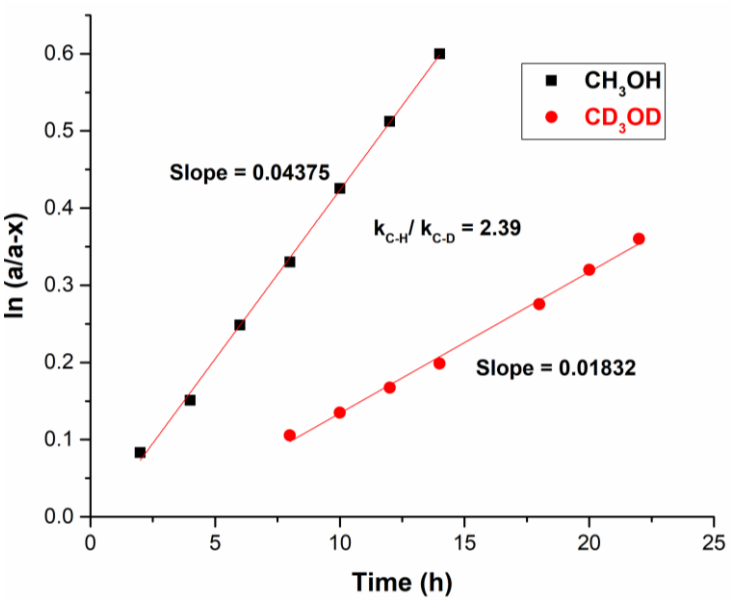

Figure S2. Determination of kinetic isotope effect for the conversion of 1-phenylpropanol.

3. Synthesis of Ru(II) hydride

3.1 Generation of Ru(II) hydride in presence of $LiHBEt_3$

In a screw cap tube, complex **B** (0.01 mmol), $LiHBEt_3$ (0.05 mmol) were added under argon and dichloromethane (1 mL) was added. The mixture was stirred at room temperature for 5 minutes. Then the solvent was evaporated under vacuum. Then ^{1}H and ^{31}P NMR spectra were recorded in benzene-D_6. The ^{1}H-NMR spectrum of **B´** showed a triplet with a characateristic peak of Ru(II)-hydride located at δ = −7.37 ppm. **^{1}H NMR** (500 MHz, benzene-D_6): δ = -7.37 (t, $J_{H,P}$ = 25.0 Hz, 1H). Also an indicative peak at δ = 56.3 ppm in ^{31}P {^{1}H} NMR spectrum was observed. **$^{31}P\{^{1}H\}$ NMR** (202 MHz, benzene-D_6): δ = 56.3.

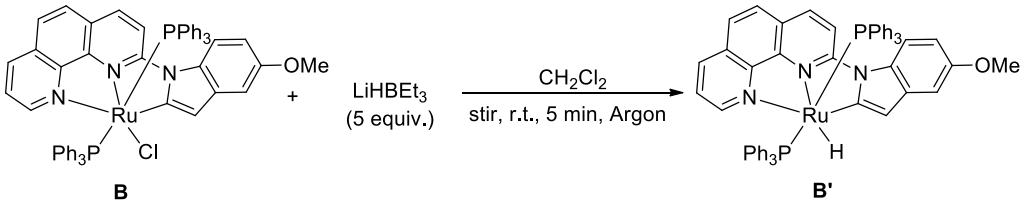

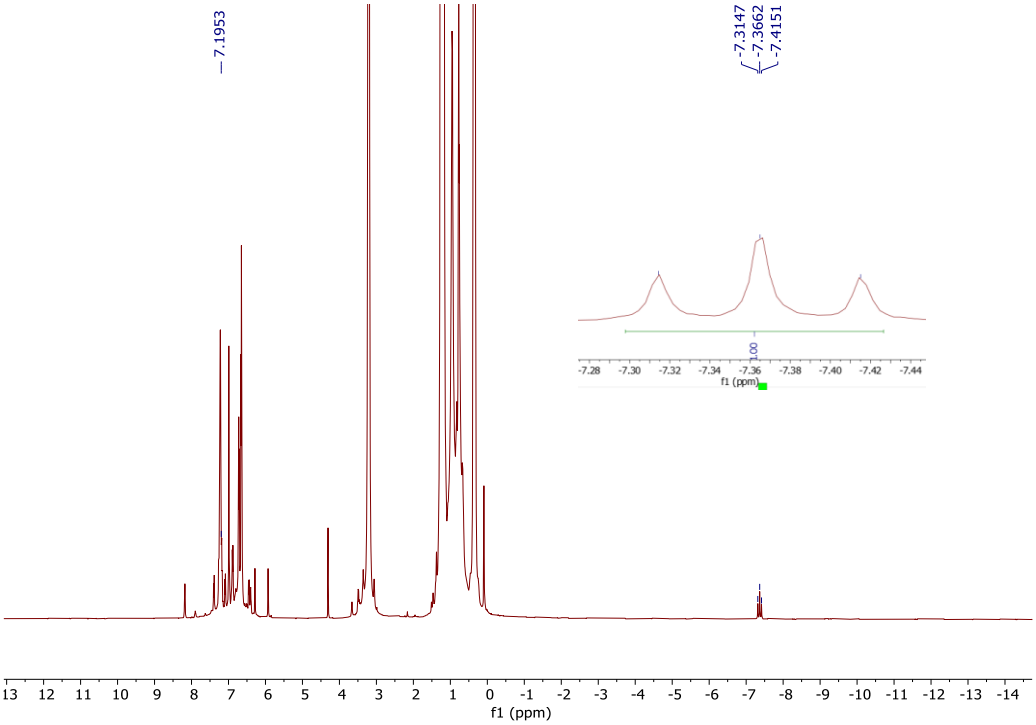

Figure S3. ^{1}H NMR spectrum of **B´** in benzene-D_6.

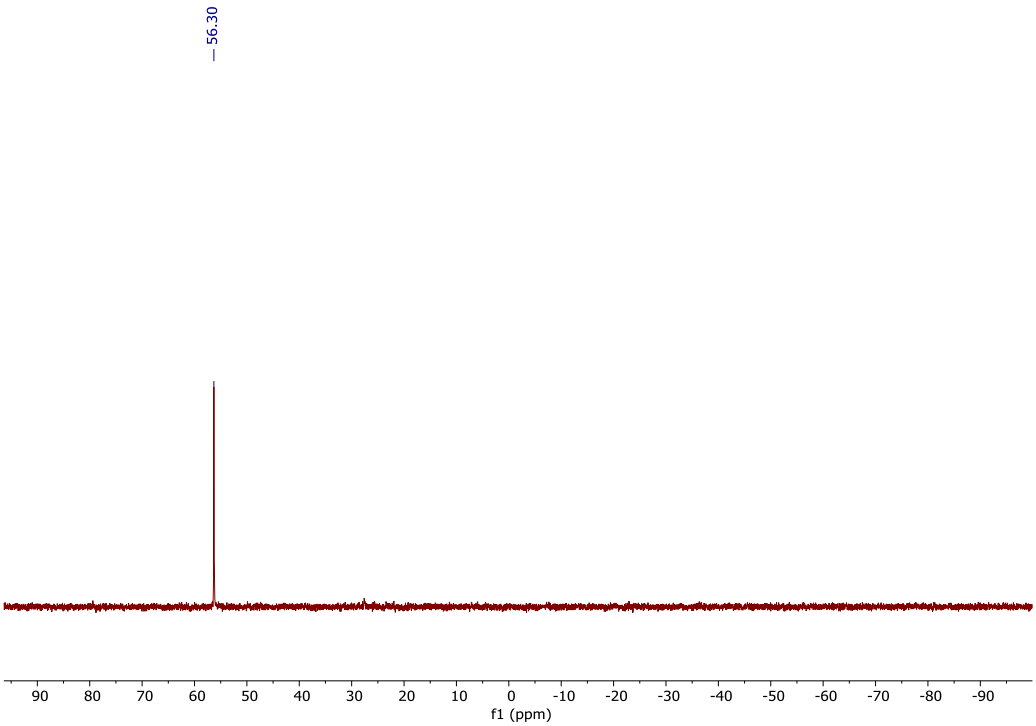

Figure S4. ^{31}P NMR spectrum of **B´** in benzene-D_6.

3.2a *In-situ* generation of Ru(II) hydride

In a screw cap tube, complex **B** (0.01 mmol), Cs_2CO_3 (0.5 mmol) and MeOH:toluene (1:1, total volume 5.0 mL) were taken and heated at 140 °C for 1 h under argon atmosphere. After that the solvent was removed under vacuum. The crude reaction mixture was dissolved in distilled dichloromethane and filtered through a cotton pad. The solvent was evaporated and then ^{1}H

NMR and ^{31}P NMR spectra were recorded in benzene-D_6. Similar to complex **B´** obtained upon treatment of **B** with $LiHBEt_3$, the ^{1}H NMR spectrum of the reaction mixture showed a peak located at δ = −7.36 ppm which indicated the *in-situ* generation of Ru(II)-hydride. **^{1}H NMR** (500 MHz, benzene-D_6): δ = -7.36 (t, $J_{H,P}$ = 25.0 Hz, 1H). In ^{31}P NMR spectrum along with few unknown signals a peak at δ = 56.1 ppm was observed which confirmed the formation of Ru(II)-hydride complex similar to **B´** under the reaction condition. **^{31}P{^{1}H} NMR** (202 MHz, benzene-D_6): δ = 56.1.

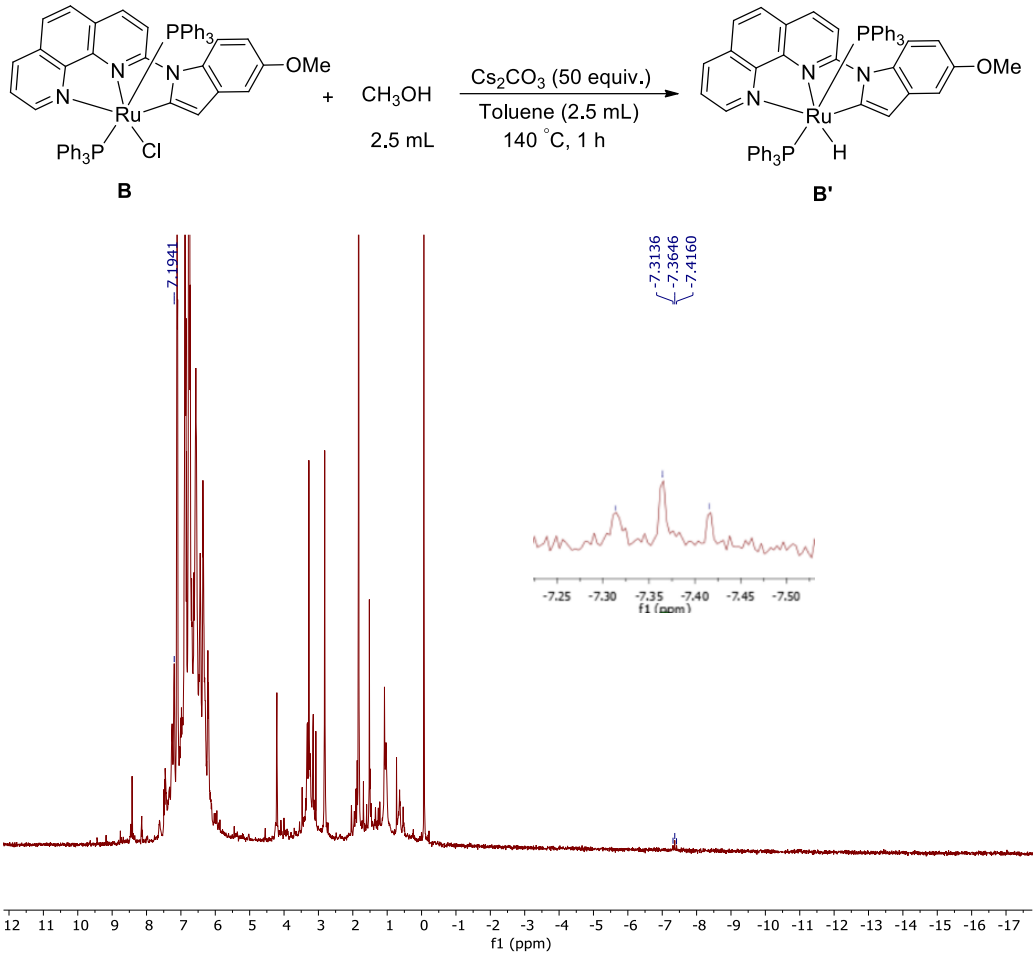

Figure S5. ^{1}H NMR spectrum of *in-situ* generated Ru(II) hydride in benzene-D_6.

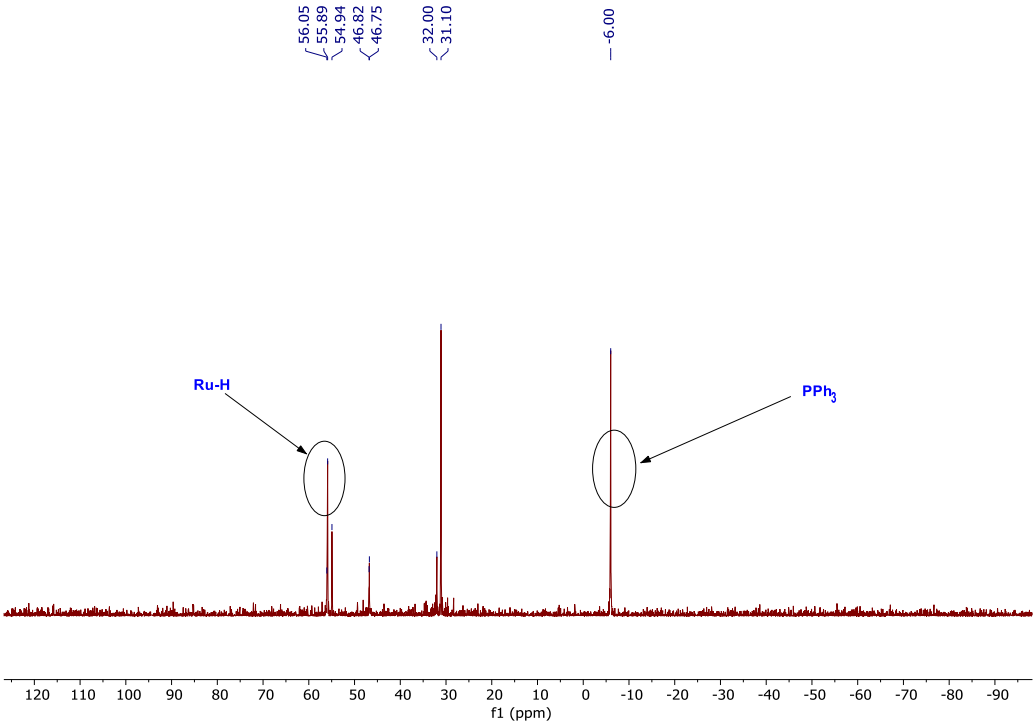

Figure S6. ^{31}P NMR spectrum of *in-situ* generated Ru(II) hydride in benzene-D_6.

3.2b Utilizing *in-situ* generated Ru(II)-hydride (B)´ for the β-methylation of 1-phenylpropanol:

In a screw cap tube, complex **B** (0.01 mmol) was taken and the tube was placed inside the glovebox. Then $LiHBEt_3$ (0.05 mmol, 1M in THF) was added and the solution was stirred for 5 minutes. Then 1-phenylpropanol (2.0 mmol), Cs_2CO_3 (2.0 mmol) and MeOH:toluene (1:1, total volume 20 mL) were taken and heated at 140 °C for 24 h under argon atmosphere. Then the tube was cooled to room temperature and 10 µL solution was syringed out for GC and GC-MS analysis. The yield of the product **4** (81%) was determined by GC analysis using mesitylene as internal standard.

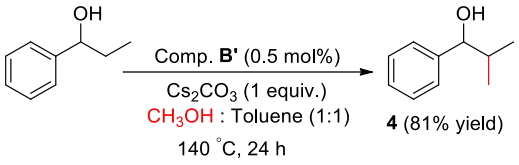

3.2c *In-situ* detection of Ru(II)-methoxide intermediate

In order to gain an insight into the catalytically active intermediates, complex **B** was heated under the reaction conditions similar to that shown under heading **3.2a**. After heating at 140 °C for 10 minutes, 20 µL aliquot was taken from the reaction mixture and submitted for ESI-MS analysis. The ESI-MS spectrum showed a peak at m/z 982.1939 which matched with the mass corresponding to complex **i [Ru-OMe + H]$^+$**. ESI-MS: Calcd. for $C_{58}H_{48}N_3O_2P_2Ru$, $[M+H]^+$: 982.1947; found: 982.1939. The observed mass and the isotopic pattern for the Ru-methoxide complex **i** (Figure **S7**, right) showed good correspondence with the simulated pattern (Figure **S7**, left).

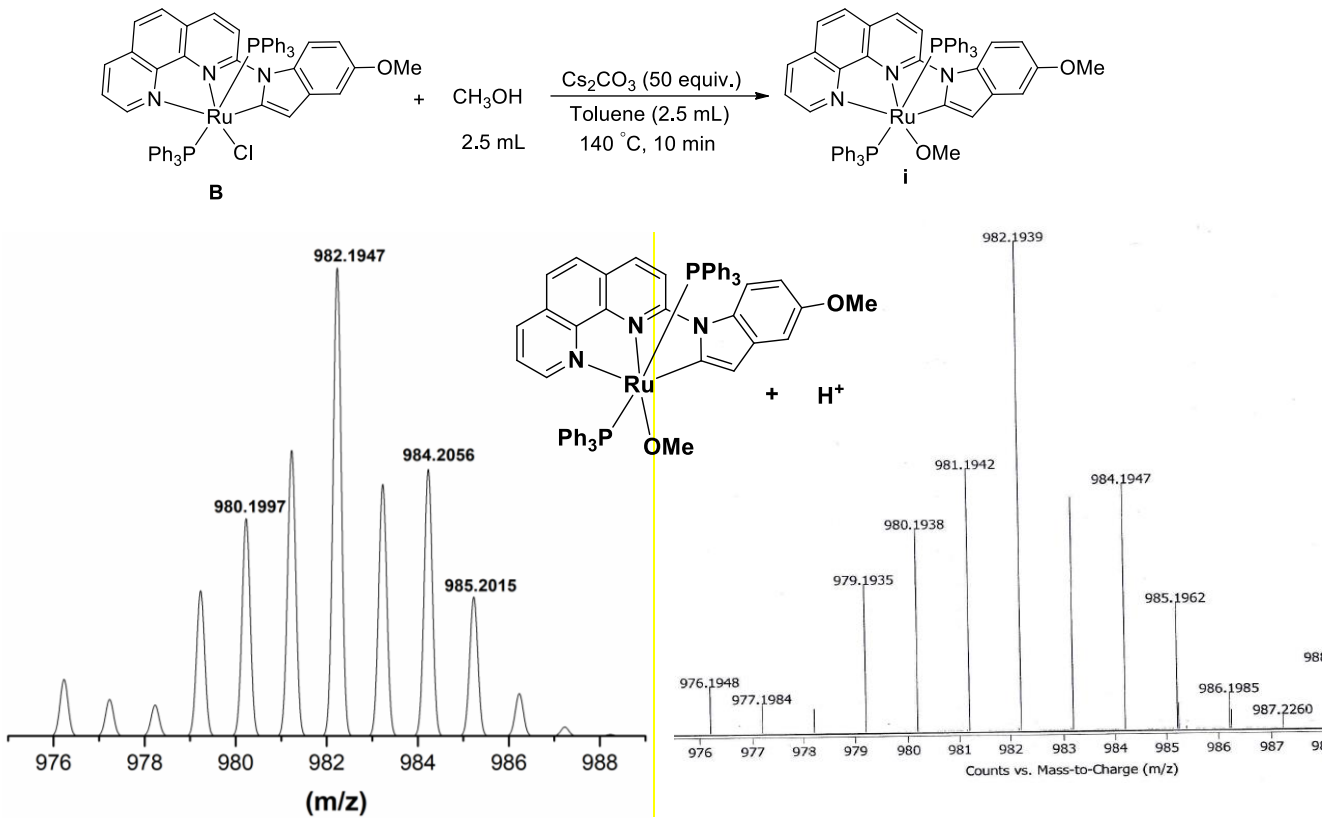

Figure S7. The ESI-MS spectrum of *in-situ* generated Ru(II)-methoxide complex. Calculated isotope patterns (left) and observed patterns (right) of generated [Ru-OMe + H^+].

4. X-Ray crystallographic studies

Single crystals of both complexes **A** and **B** were obtained by slow evaporation of a saturated solution of the respective complexes in DCM-Et_2O mixture. Single crystal X-ray data of the complexes were collected at 100 K by using a Bruker SMART APEX II CCD diffractometer and Bruker D8 Quest Single Crystal diffractometer with graphite monochromated MoKα radiation (λ =0.71073 Å). The frames were indexed, integrated and scaled using SMART and SAINT software package and the data were corrected for absorption using the SADABS program. The structures were solved and refined using WINGX, Olex2 and SHELX programs. The crystallographic figures have been generated using Diamond 3 software10 (30% probability thermal ellipsoids). The CCDC number of complexes **A** and **B** are 2103768 and 1966587 respectively.

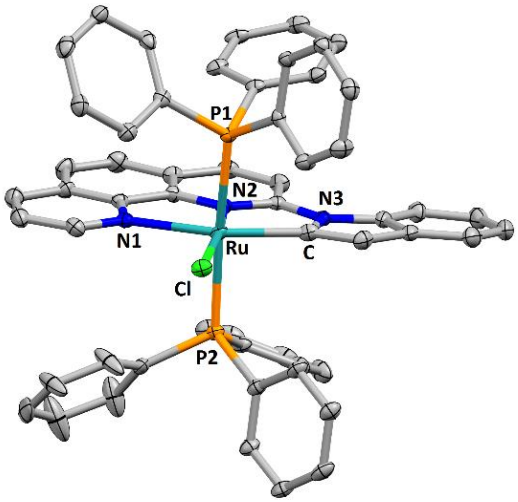

Figure S8. Solid state structure of complex **A** (30 % thermal ellipsoids; hydrogen atoms were omitted for clarity).

Table S1. Crystal data and structure refinement for complex **A**.

Formula	'$C_{56}H_{42}ClN_3P_2Ru$'
Formula weight	955.38
Crystal colour, habit	Brown, prism
T / K	100(2)
Crystal system	Monoclinic
Space group	*P-121/n* (no. 14)
a/Å	13.390(2)
b/Å	22.927(4)
c/Å	16.646(3)
α/°	90
β/°	99.647(5)
γ/°	90
V/Å^3	5038.0(14)

Z	4
D_c/g cm^{-3}	1.260
μ/mm^{-1}	0.466
Reflections measured	12498
Unique reflections	7336
Reflections used $I > 2\sigma(I)$]	75666
$R_1{}^a$, $wR_2{}^b$ [$I > 2\sigma(I)$]	R_1 = 0.0674^a wR_2 = 0.1652^b
$R_1{}^a$, $wR_2{}^b$(all data)	R_1=0.1289^a wR_2=0.2058^b
GOF on F^2	1.028

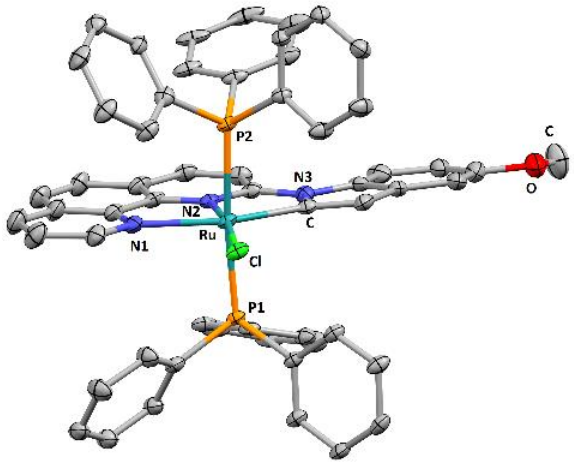

Figure S9. Solid state structure of complex **B** (30 % thermal ellipsoids; hydrogen atoms were omitted for clarity).

Table S2. Crystal data and structure refinement for complex **B**.

Formula	'C57 H44 Cl N3 O P2 Ru'
Formula weight	985.41
Crystal colour, habit	Brown, block
T / K	100(2)

Crystal system	Monoclinic
Space group	*P-121/n* (no. 14)
a/Å	13.968 (12)
b/Å	22.876 (2)
c/Å	16.645 (15)
α/°	90
β/°	101.007 (2)
γ/°	90
V/Å^3	5221.0 (8)
Z	4
Index Ranges	-16<h<16, -27<k<27, -19<l<19
F 000	2024.0
D_c/g cm^{-3}	1.254
μ/mm^{-1}	0.453
Reflections measured	9167
R_1[a], wR_2[b] [$I > 2\sigma(I)$]	$R_1 = 0.0608$[a] $wR_2 = 0.1639$[b]
R_1[a], wR_2[b](all data)	$R_1 = 0.0812$[a] $wR_2 = 0.1845$[b]
GOF on F^2	1.060

[a]$R_1 = \Sigma||F_o| - |F_c||/\Sigma|F_o|$. [b]$wR_2 = \{\Sigma[w\,(|F_o|^2 - |F_c|^2)^2]/\,\Sigma[w(|F_o|^2)^2]\}^{1/2}$

5. Copies of ^{1}H and ^{13}C NMR Spectra

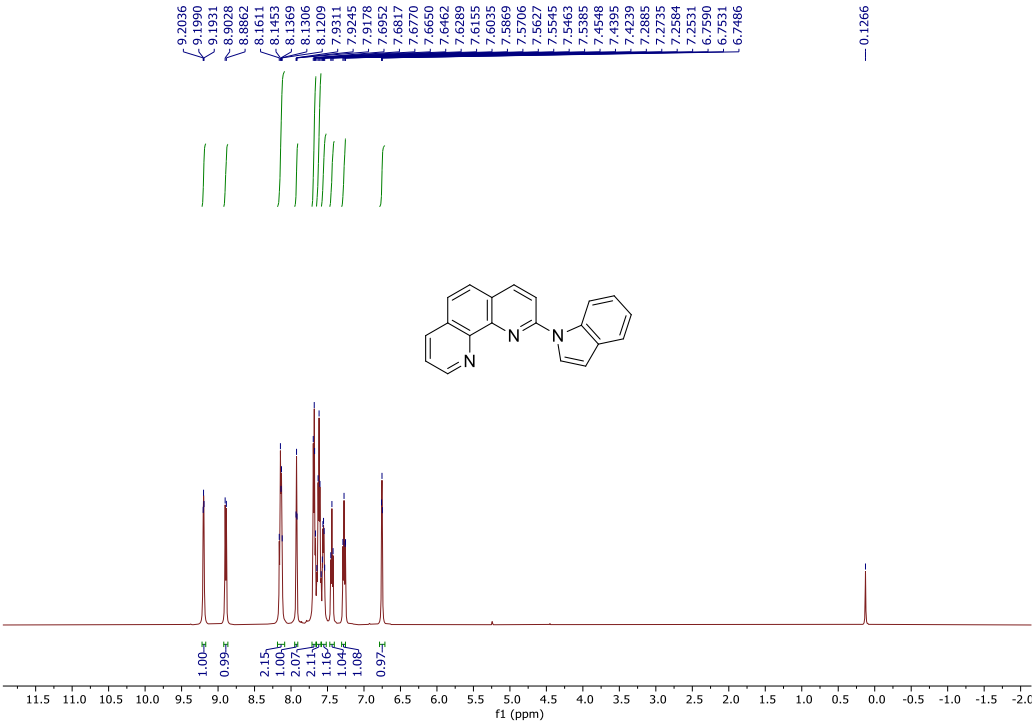

Figure S10. ^{1}H NMR Spectrum of **L_1** in $CDCl_3$.

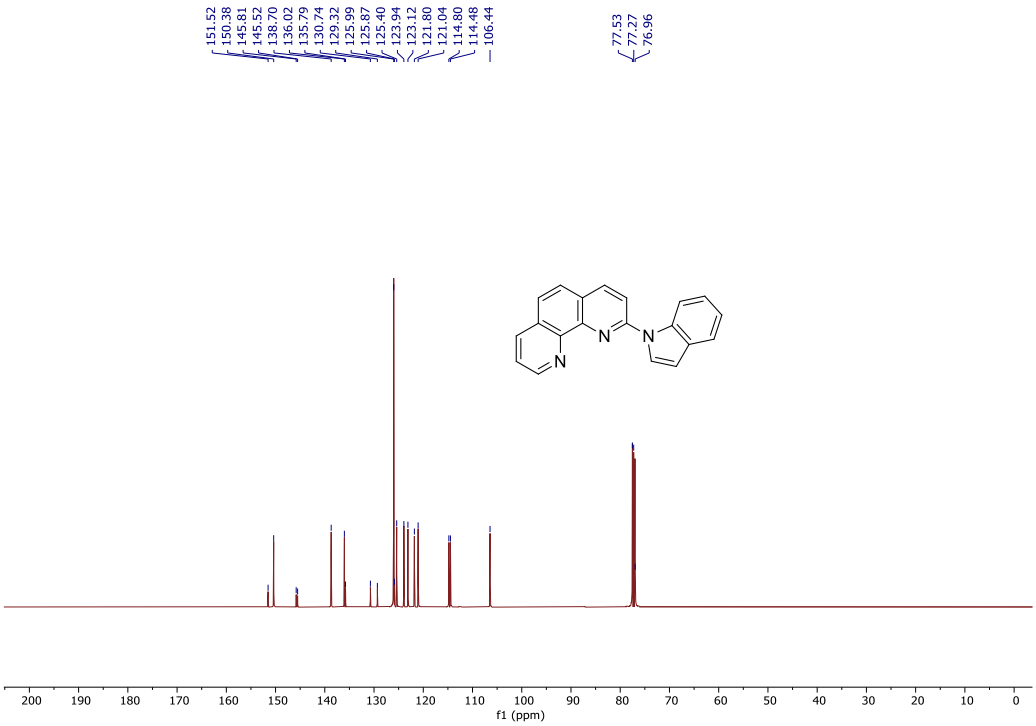

Figure S11. ^{13}C NMR Spectrum of **L_1** in $CDCl_3$.

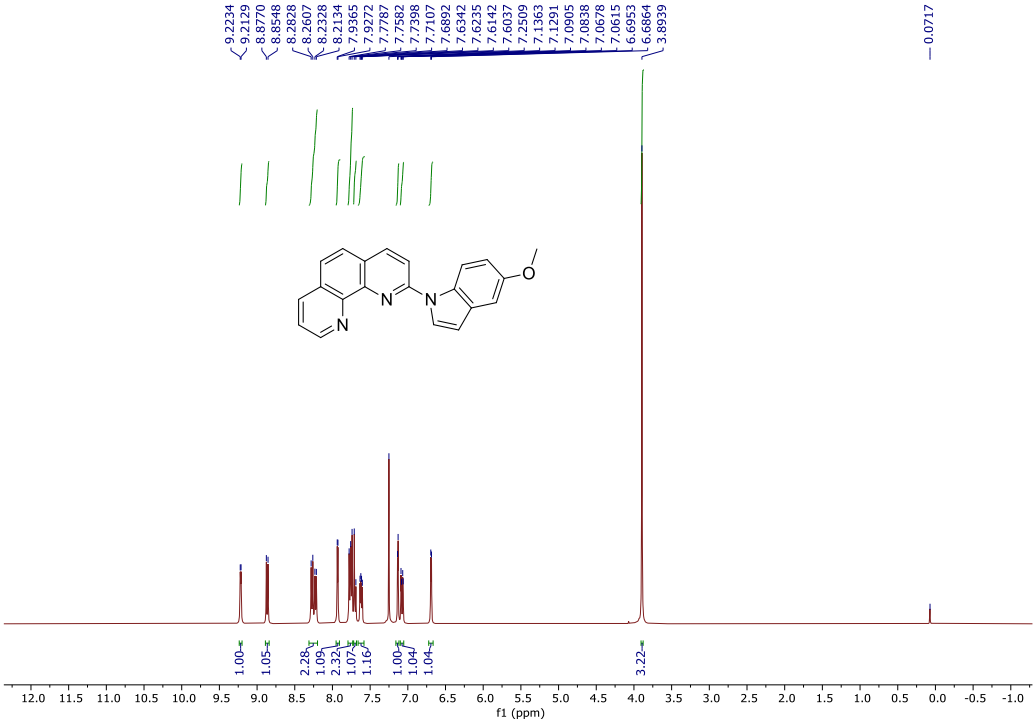

Figure S12. ^{1}H NMR Spectrum of **L2** in $CDCl_3$.

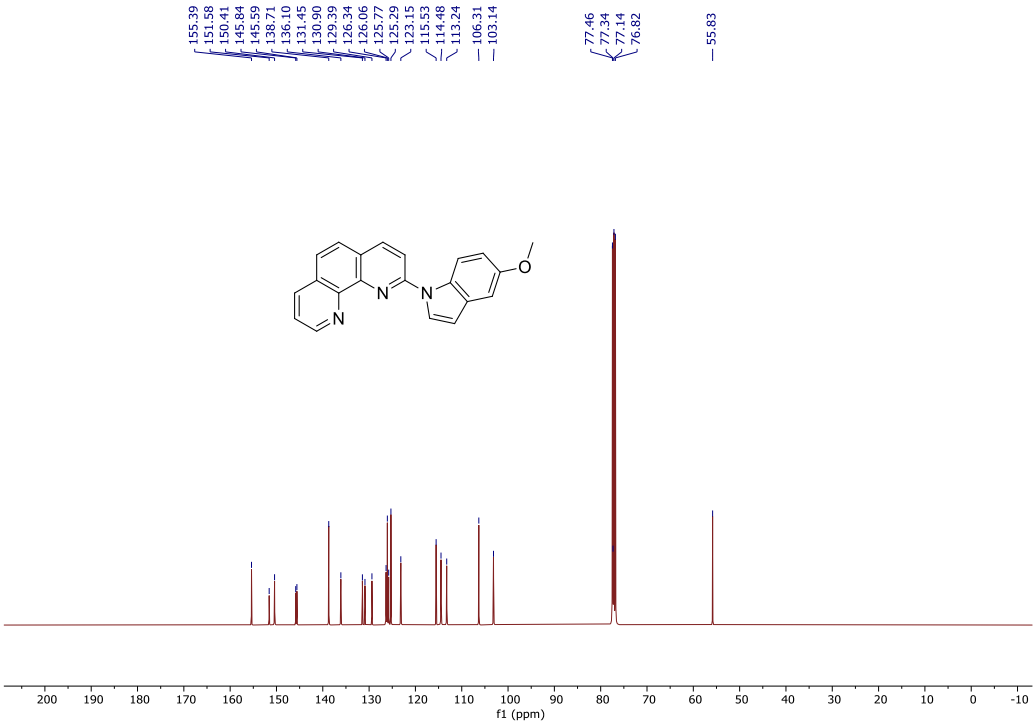

Figure S13. ^{13}C NMR Spectrum of **L2** in $CDCl_3$.

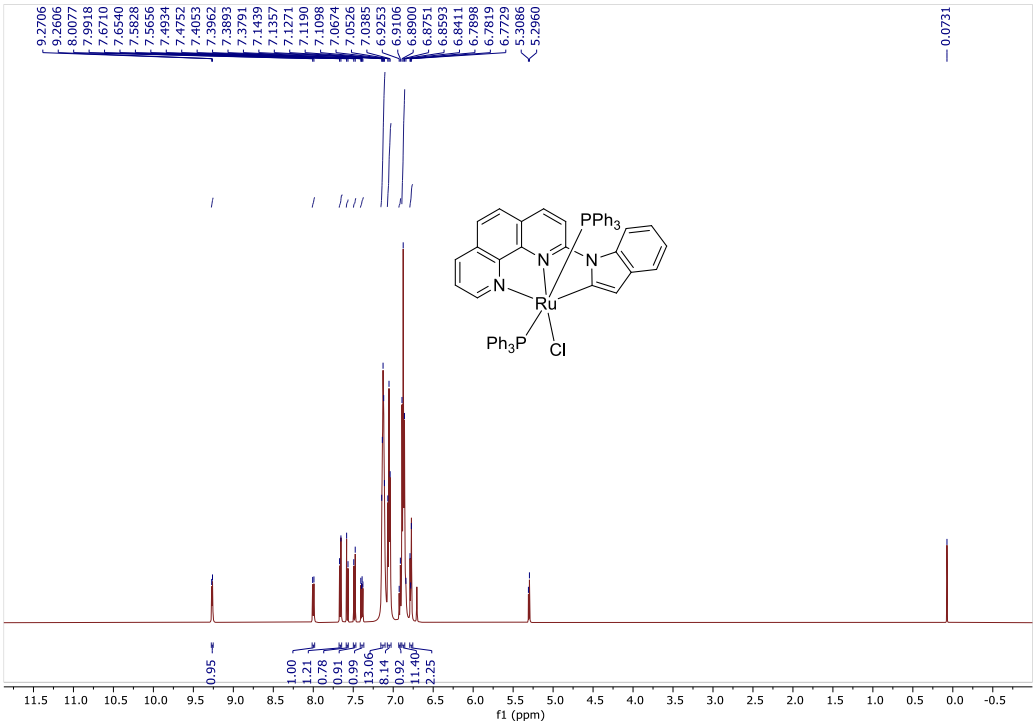

Figure S14. ^{1}H NMR Spectrum of Complex **A** in CD_2Cl_2.

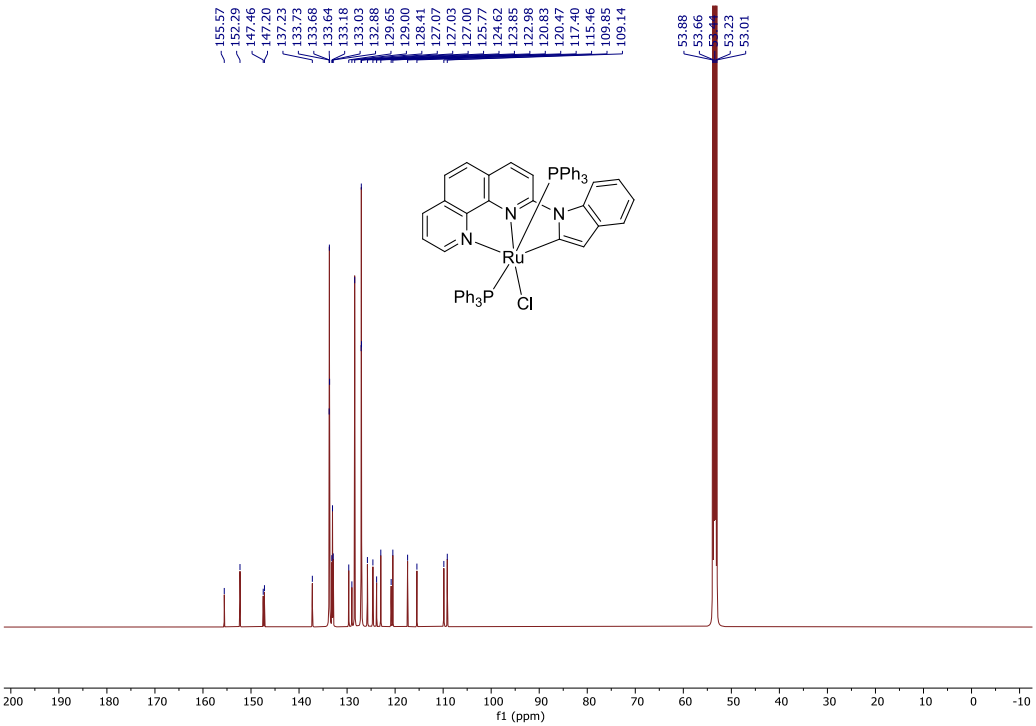

Figure S15. ^{13}C NMR Spectrum of Complex **A** in CD_2Cl_2.

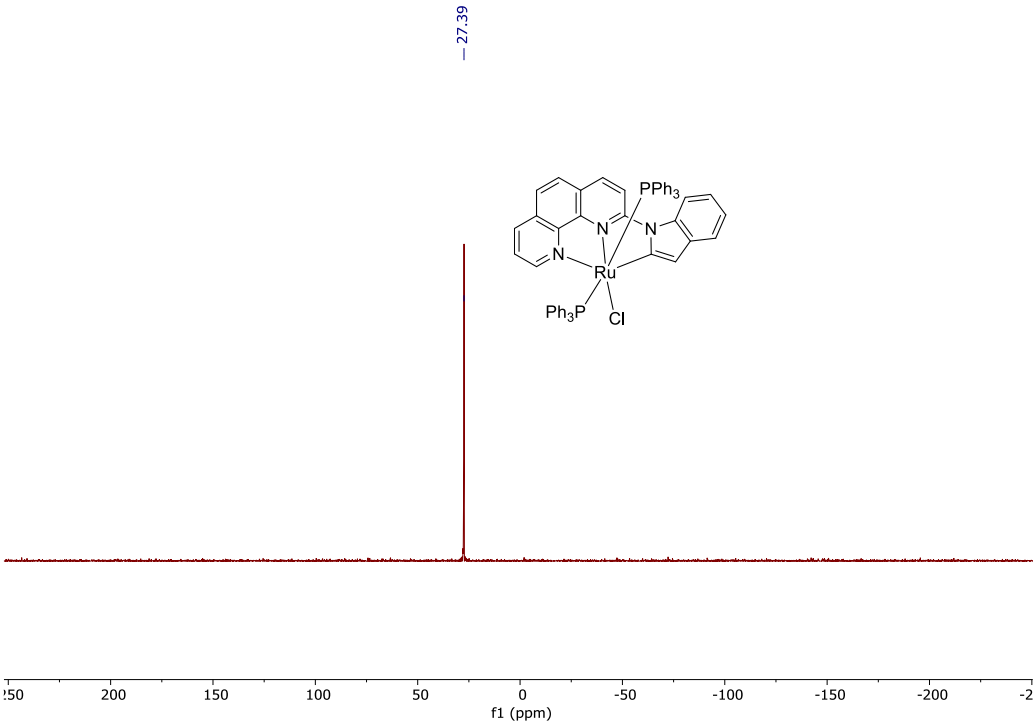

Figure S16. ^{31}P NMR Spectrum of Complex **A** in CD_2Cl_2.

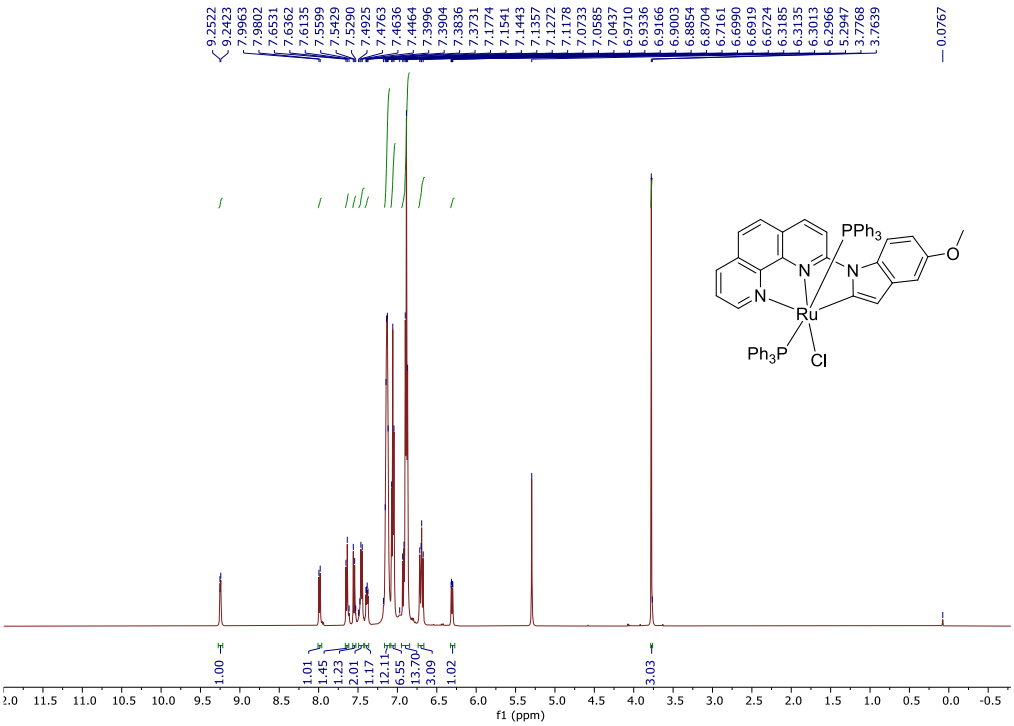

Figure S17. ^{1}H NMR Spectrum of Complex **B** in CD_2Cl_2.

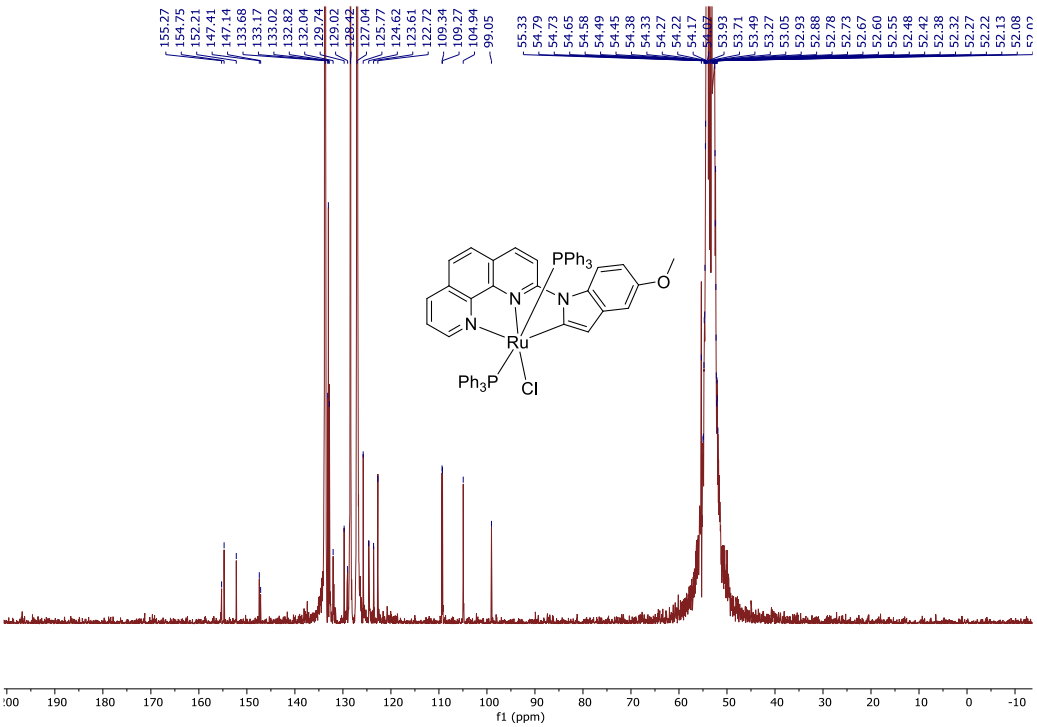

Figure S18. ^{13}C NMR Spectrum of Complex **B** in CD_2Cl_2.

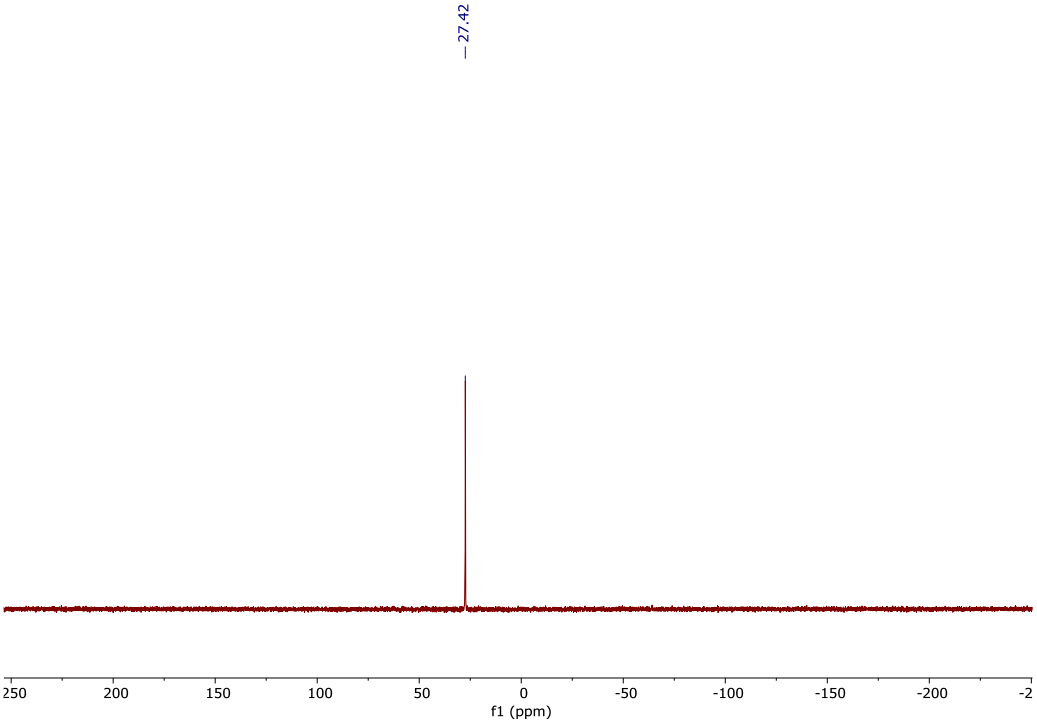

Figure S19. ^{31}P NMR Spectrum of Complex **B** in CD_2Cl_2.

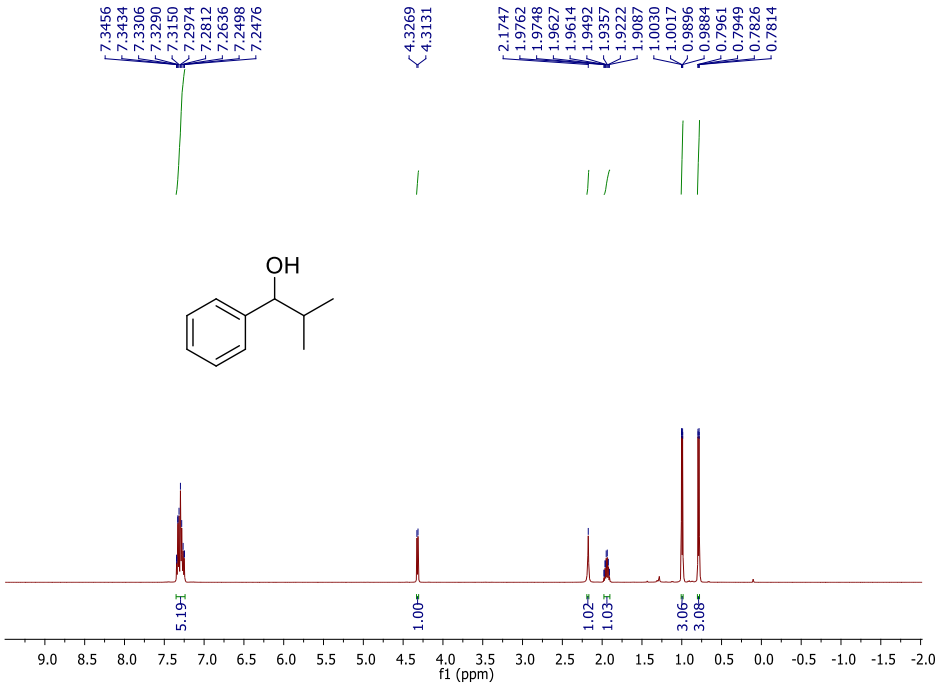

Figure S20. ^{1}H NMR Spectrum of **4** in $CDCl_3$.

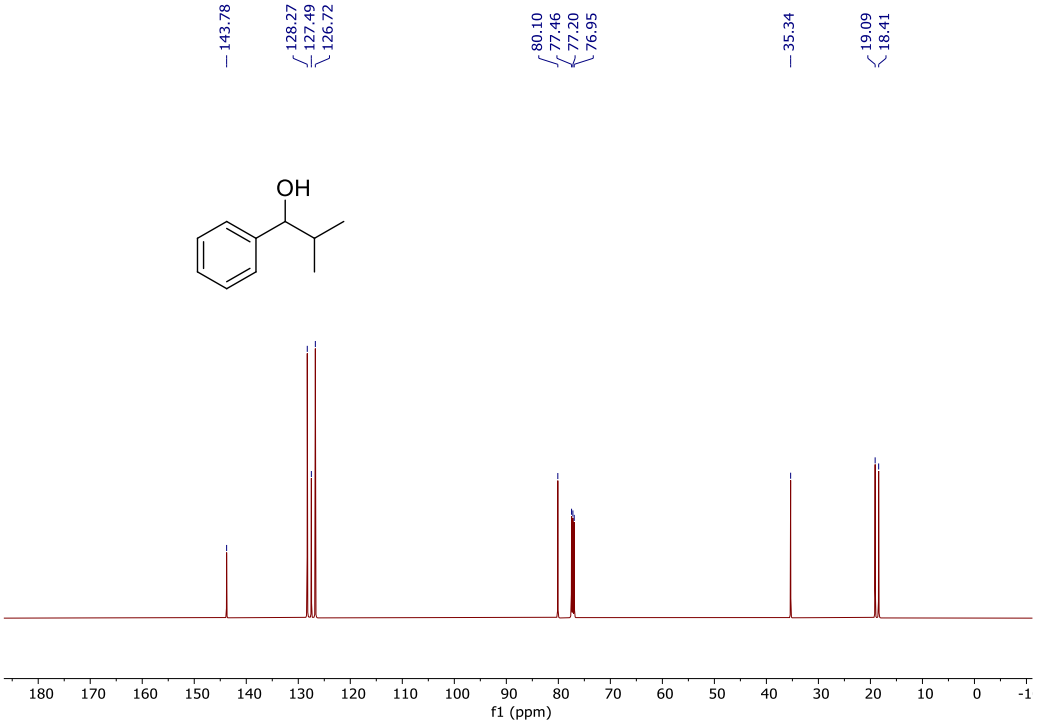

Figure S21. ^{13}C NMR Spectrum of **4** in $CDCl_3$.

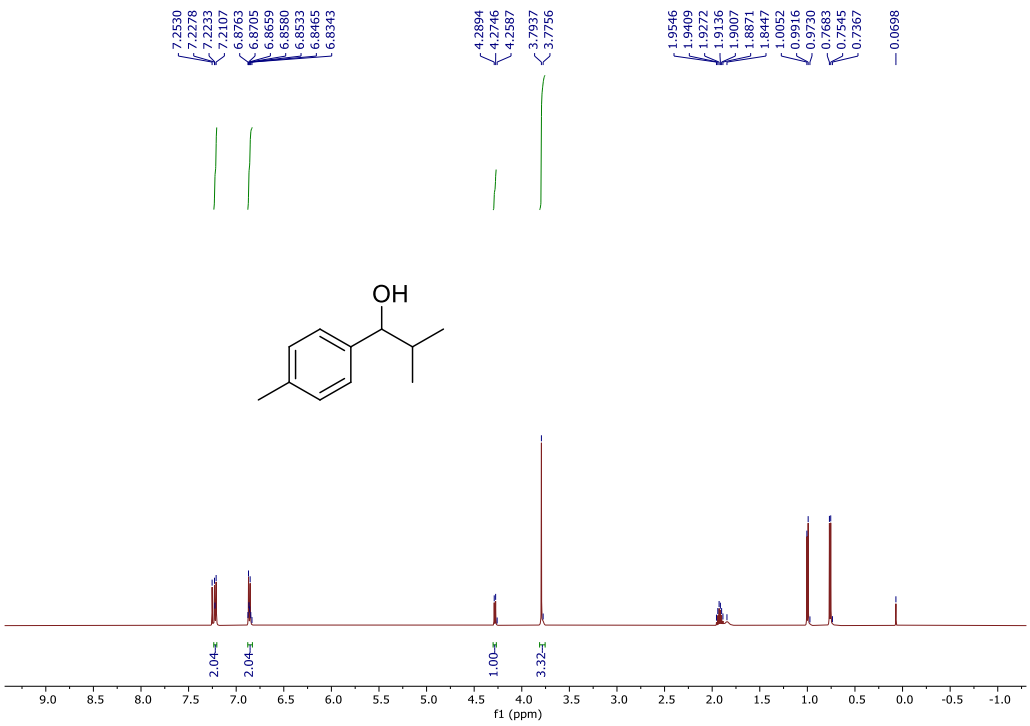

Figure S22. ^{1}H NMR Spectrum of **5** in $CDCl_3$.

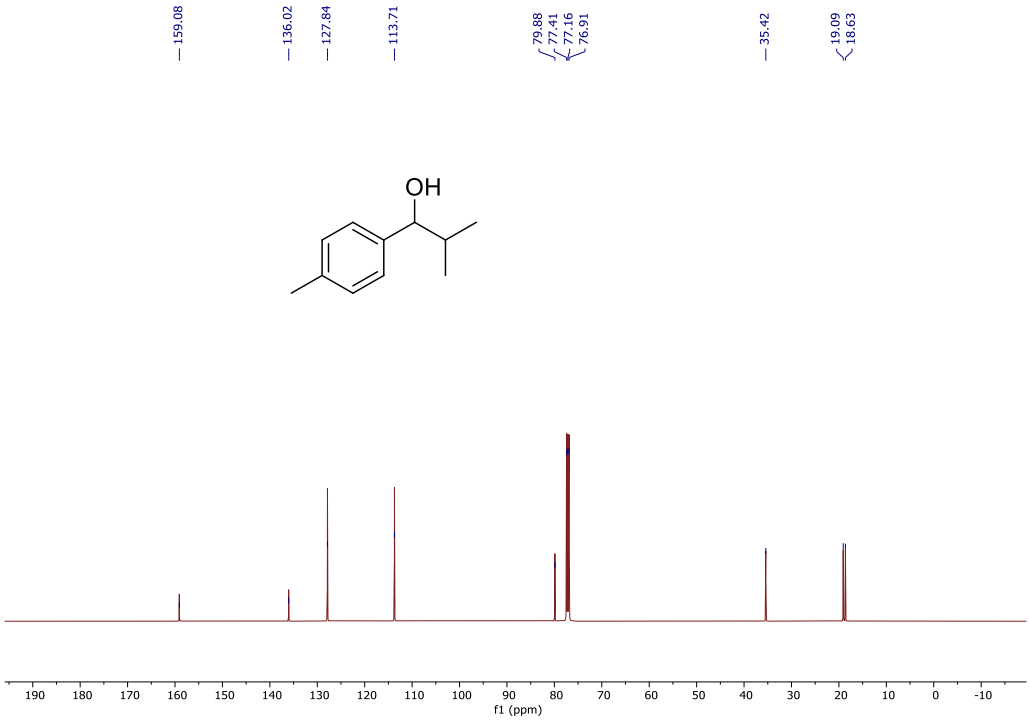

Figure S23. ^{13}C NMR Spectrum of **5** in $CDCl_3$.

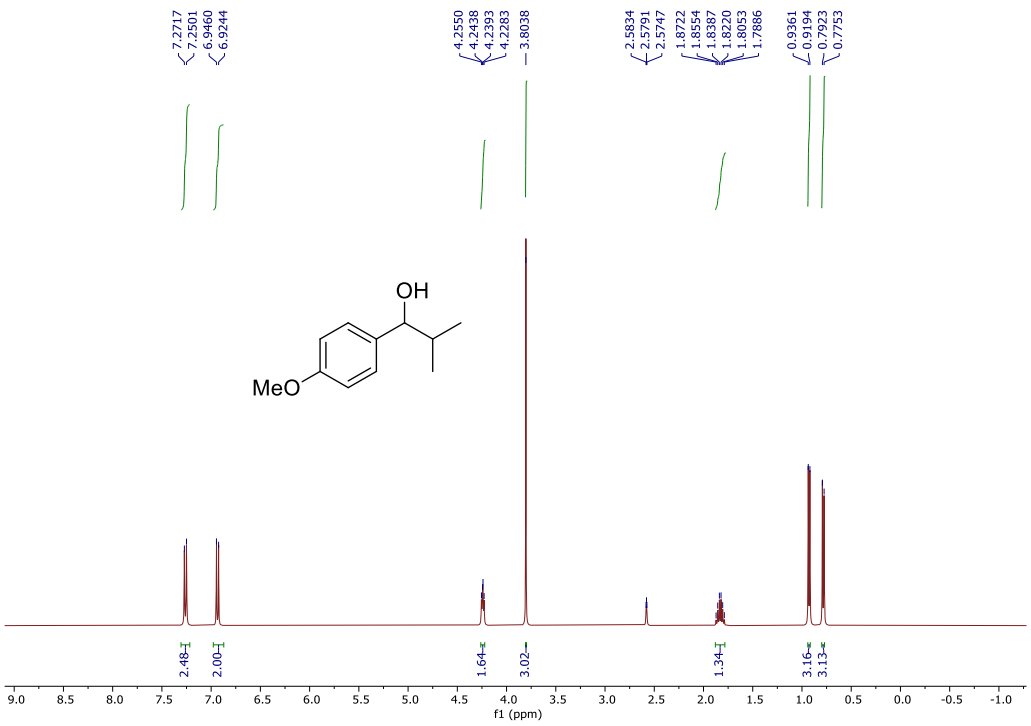

Figure S24. ^{1}H NMR Spectrum of **6** in DMSO-D_6.

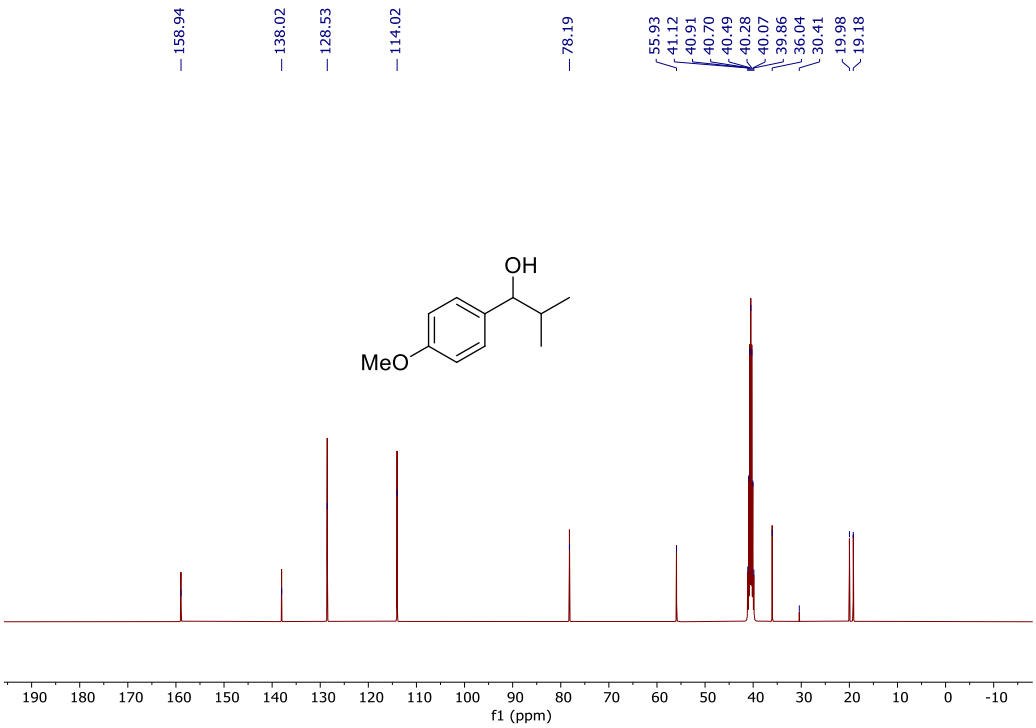

Figure S25. ^{13}C NMR Spectrum of **6** in DMSO-D_6.

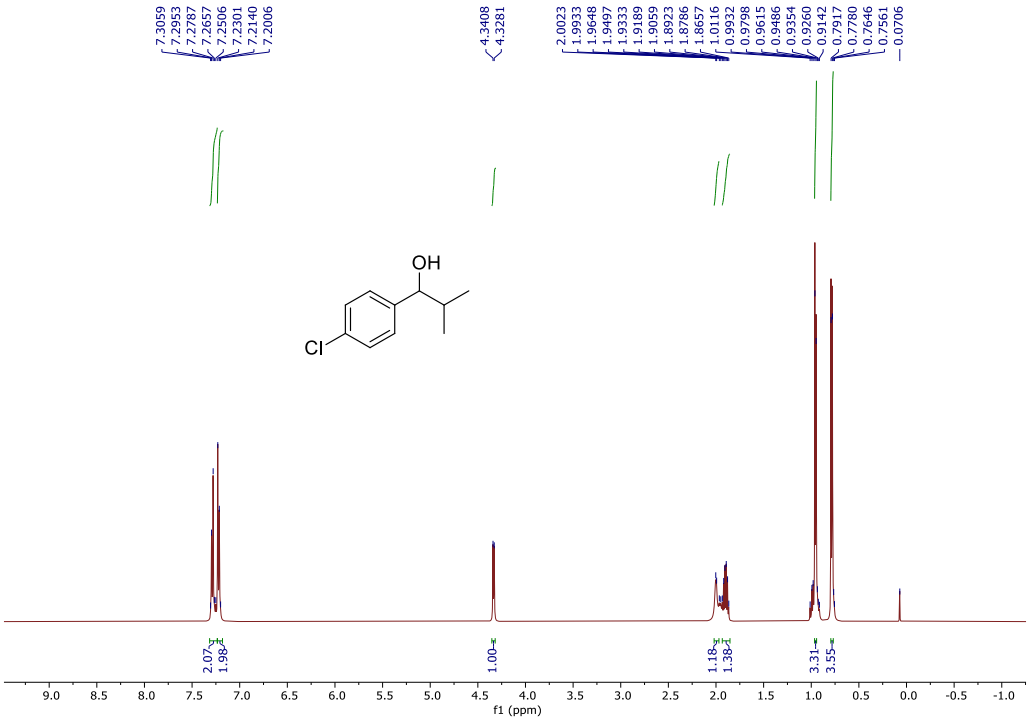

Figure S26. ^{1}H NMR Spectrum of **7** in $CDCl_3$.

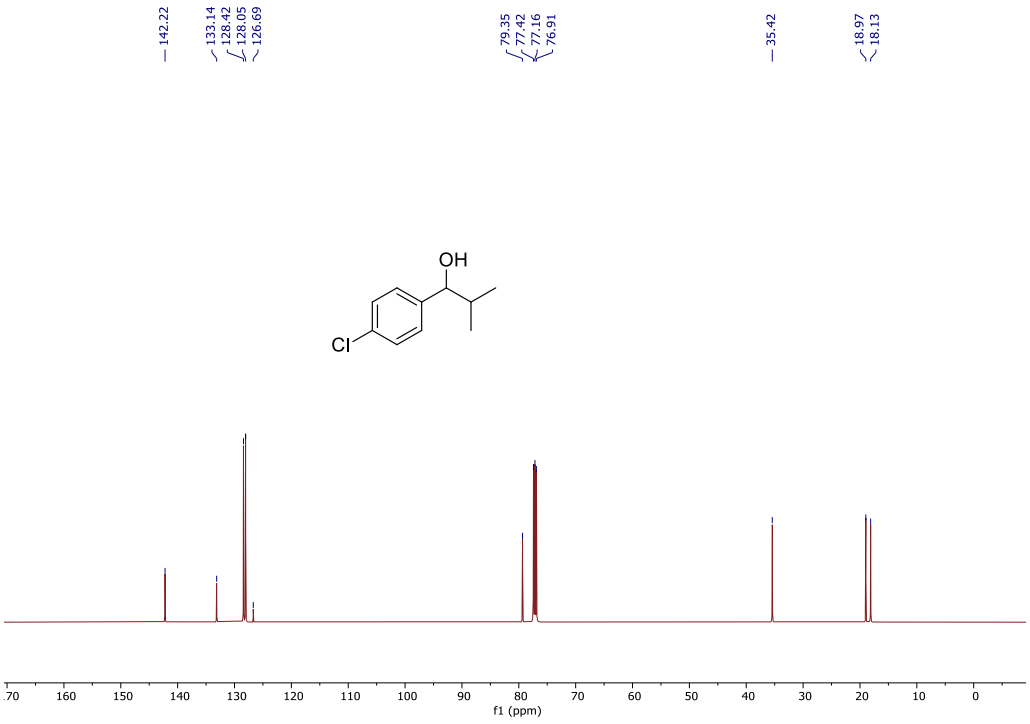

Figure S27. ^{13}C NMR Spectrum of **7** in $CDCl_3$.

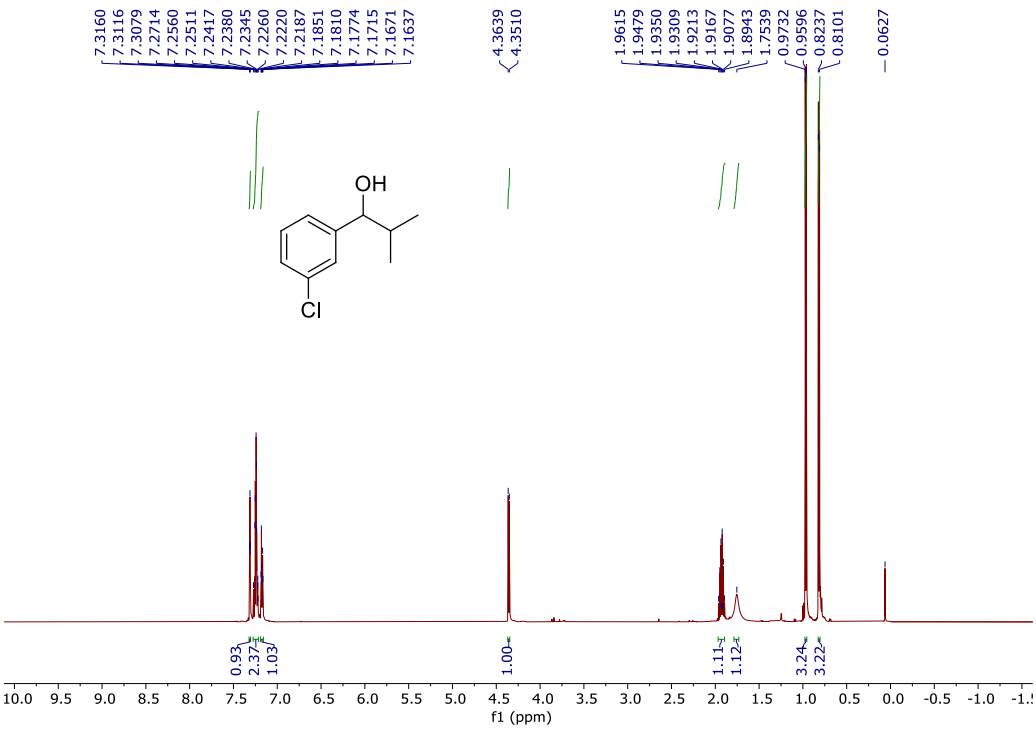

Figure S28. ^{1}H NMR Spectrum of **8** in $CDCl_3$.

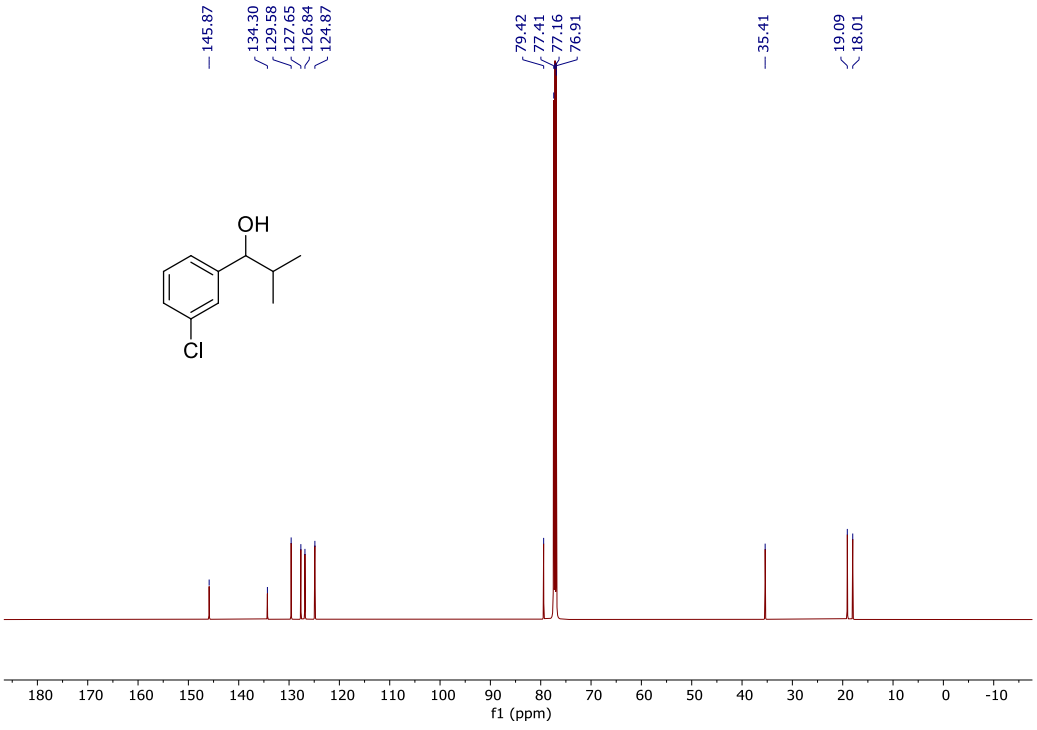

Figure S29. ^{13}C NMR Spectrum of **8** in $CDCl_3$.

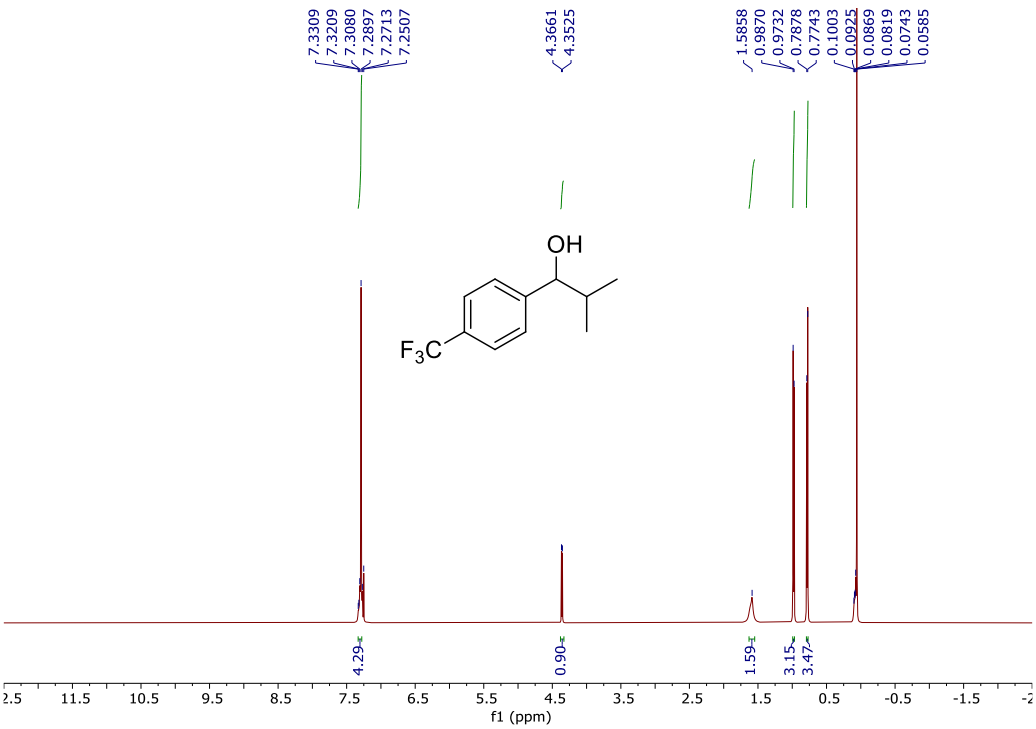

Figure S30. ^{1}H NMR Spectrum of **9** in $CDCl_3$.

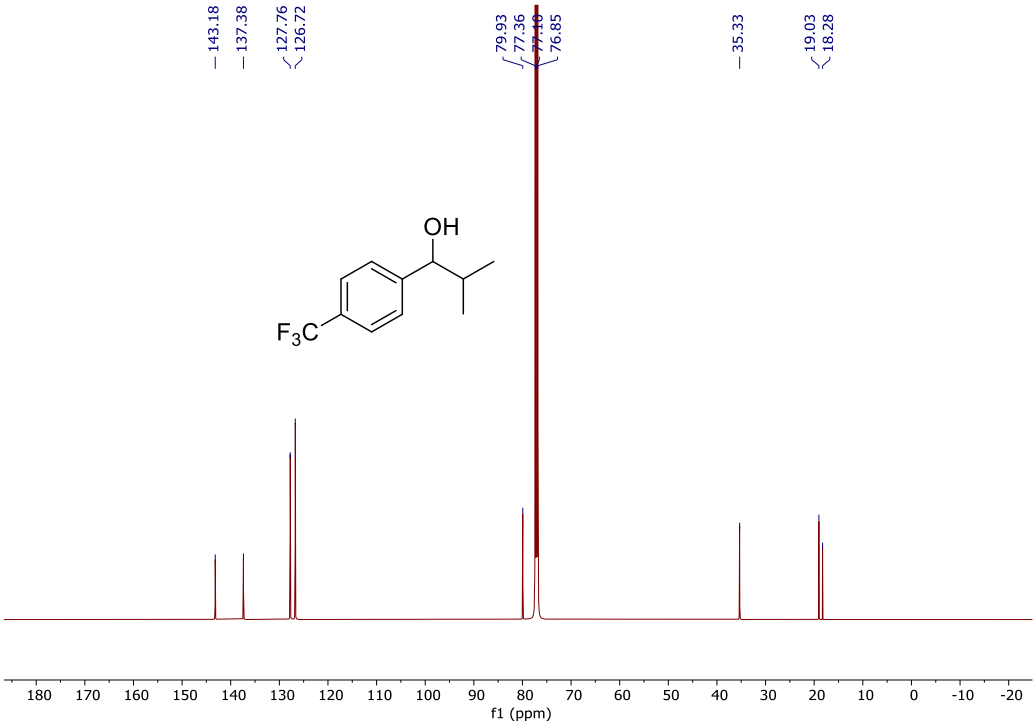

Figure S31. ^{13}C NMR Spectrum of **9** in $CDCl_3$.

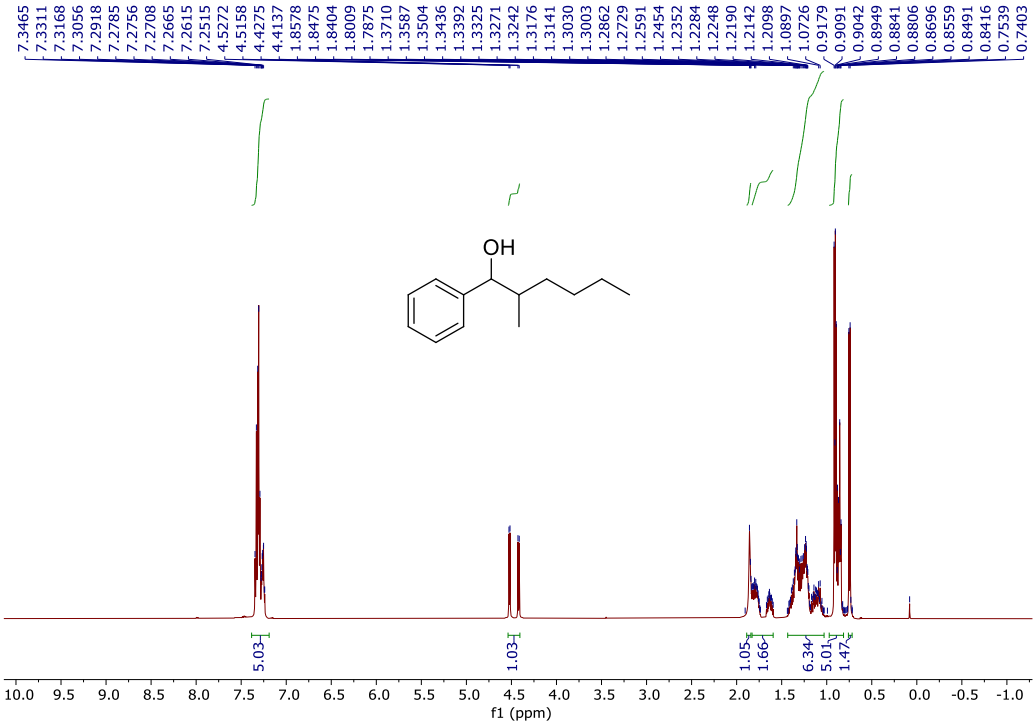

Figure S32. ^{1}H NMR Spectrum of **10** in $CDCl_3$.

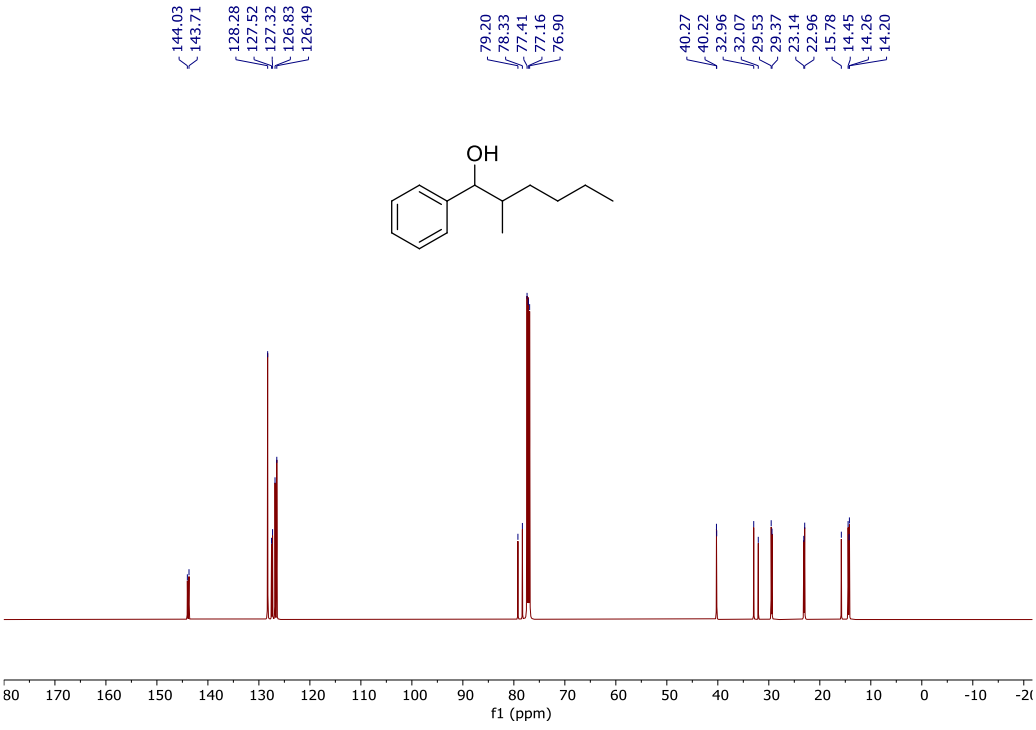

Figure S33. ^{13}C NMR Spectrum of **10** in $CDCl_3$.

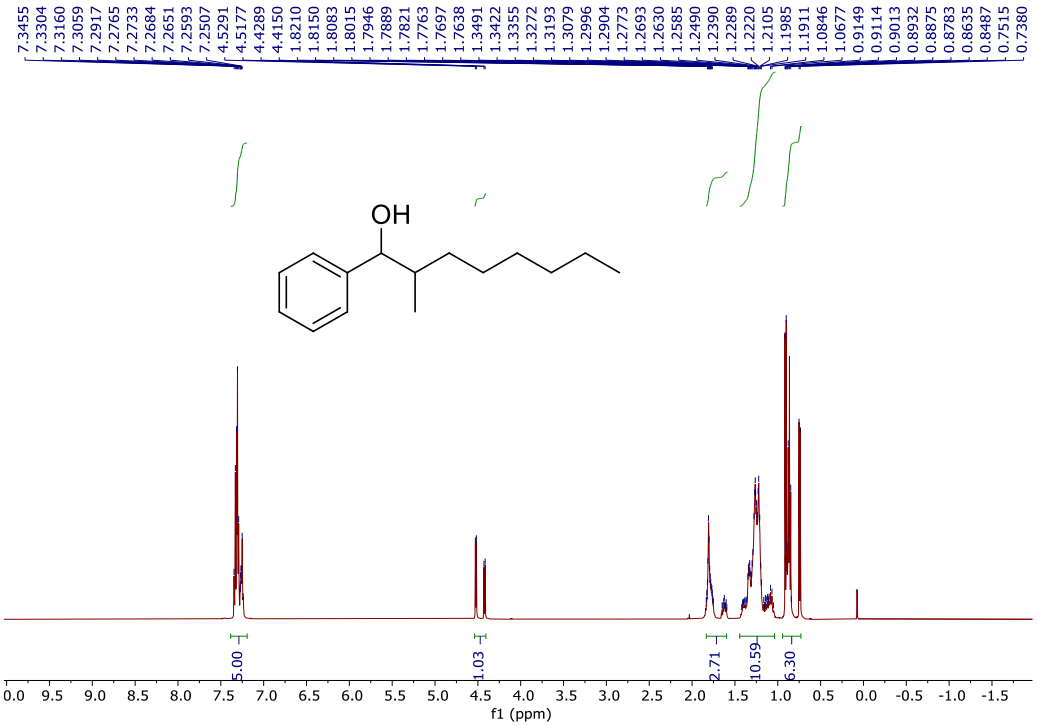

Figure S34. ^{1}H NMR Spectrum of **11** in $CDCl_3$.

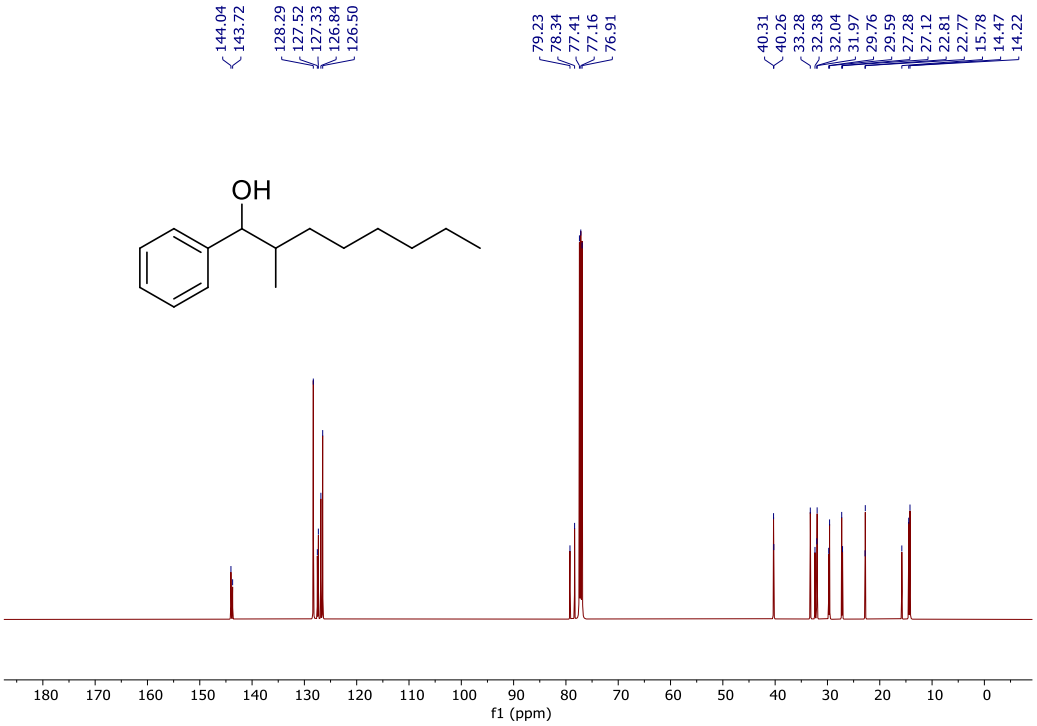

Figure S35. ^{13}C NMR Spectrum of **11** in $CDCl_3$.

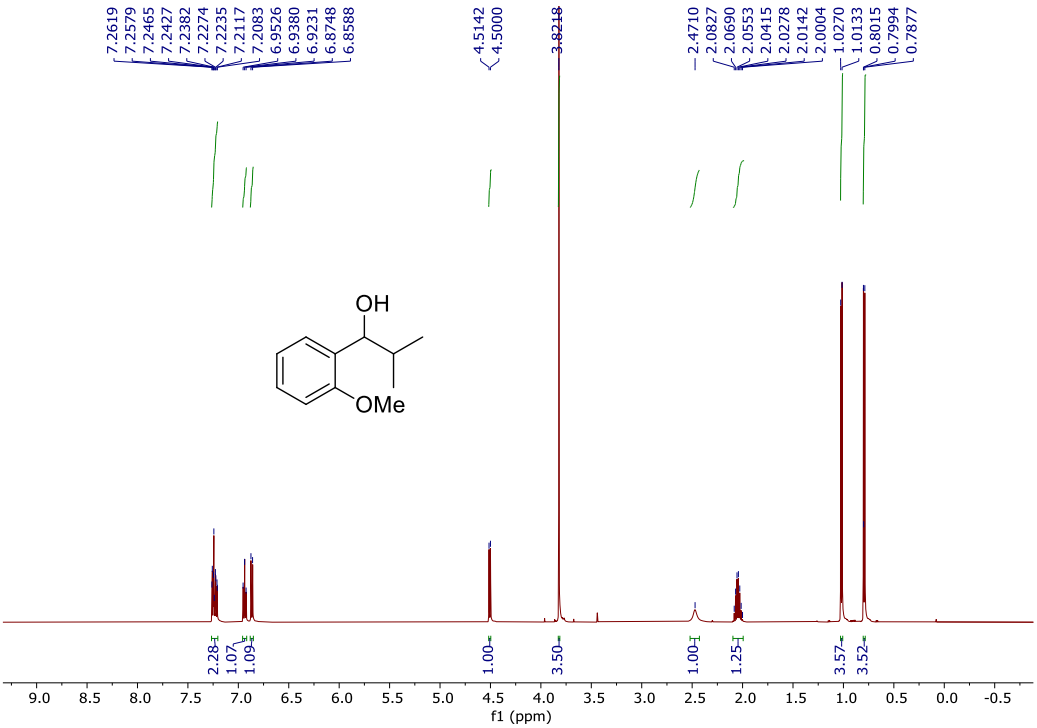

Figure S36. ^{1}H NMR Spectrum of **12** in $CDCl_3$.

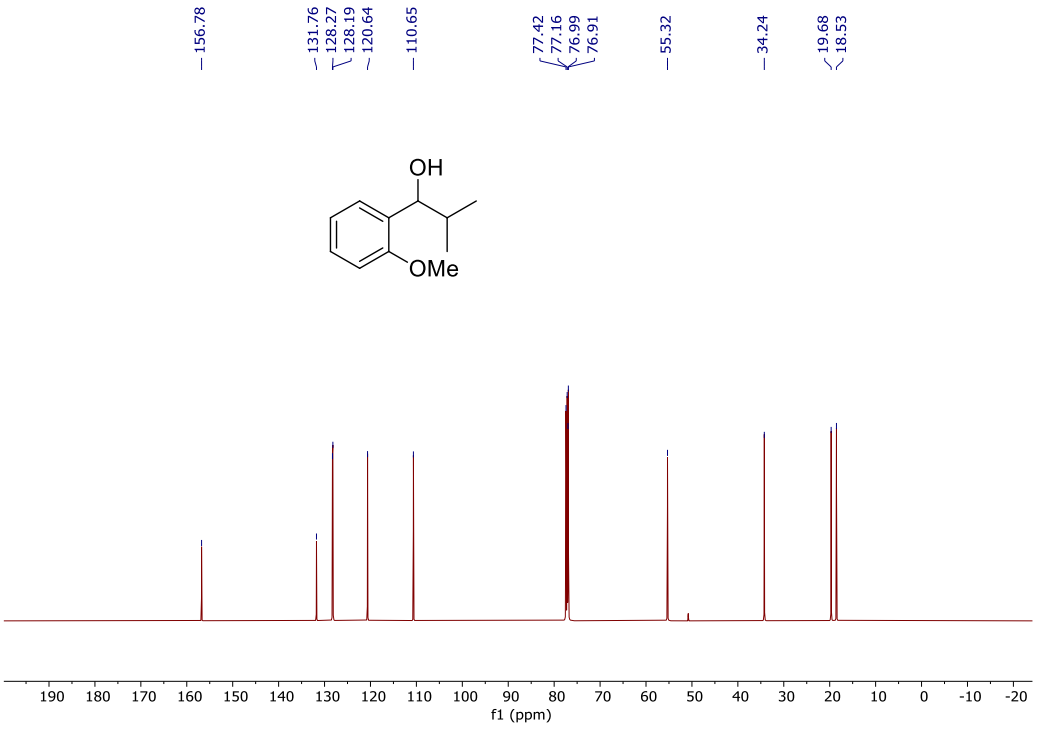

Figure S37. ^{13}C NMR Spectrum of **12** in $CDCl_3$.

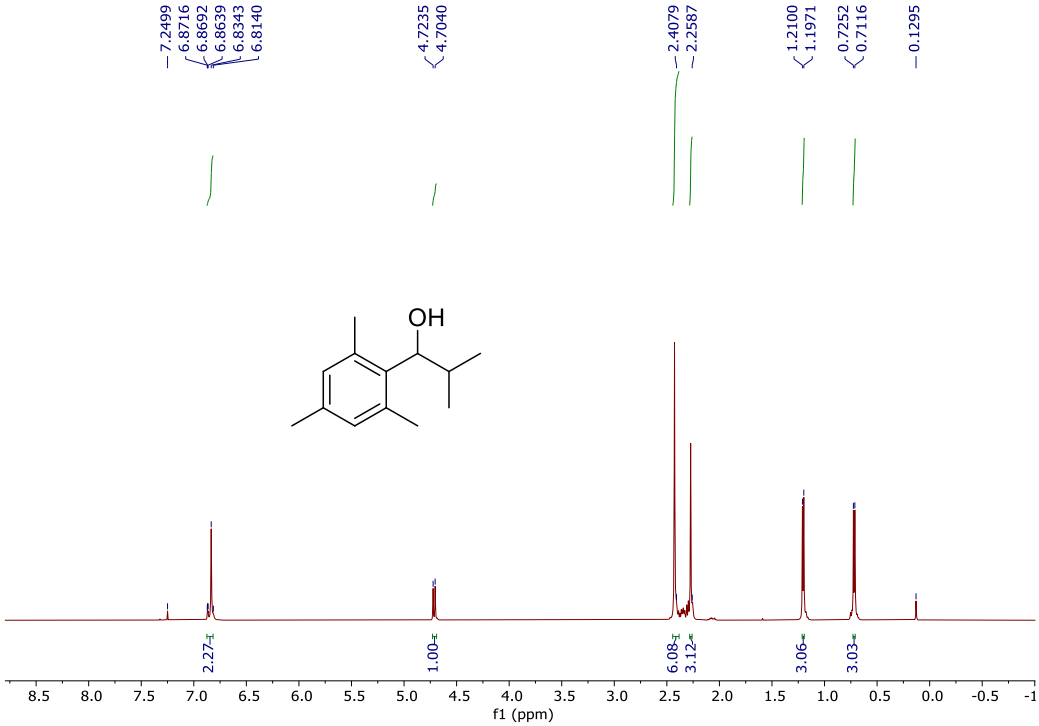

Figure S38. ^{1}H NMR Spectrum of **13** in $CDCl_3$.

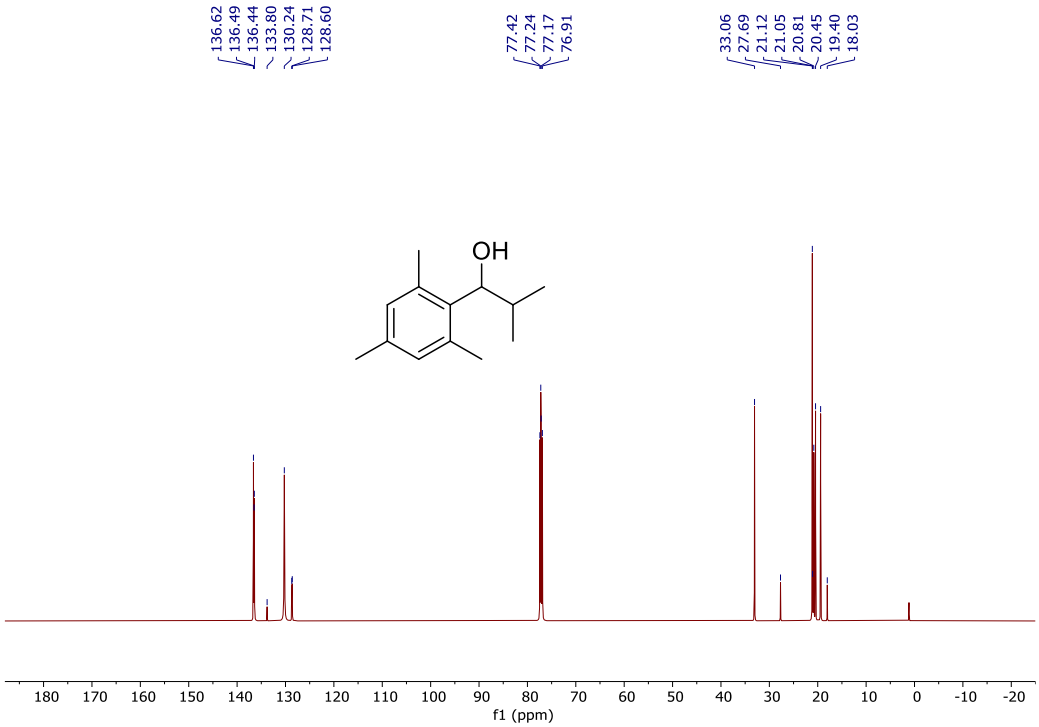

Figure S39. ^{13}C NMR Spectrum of **13** in $CDCl_3$.

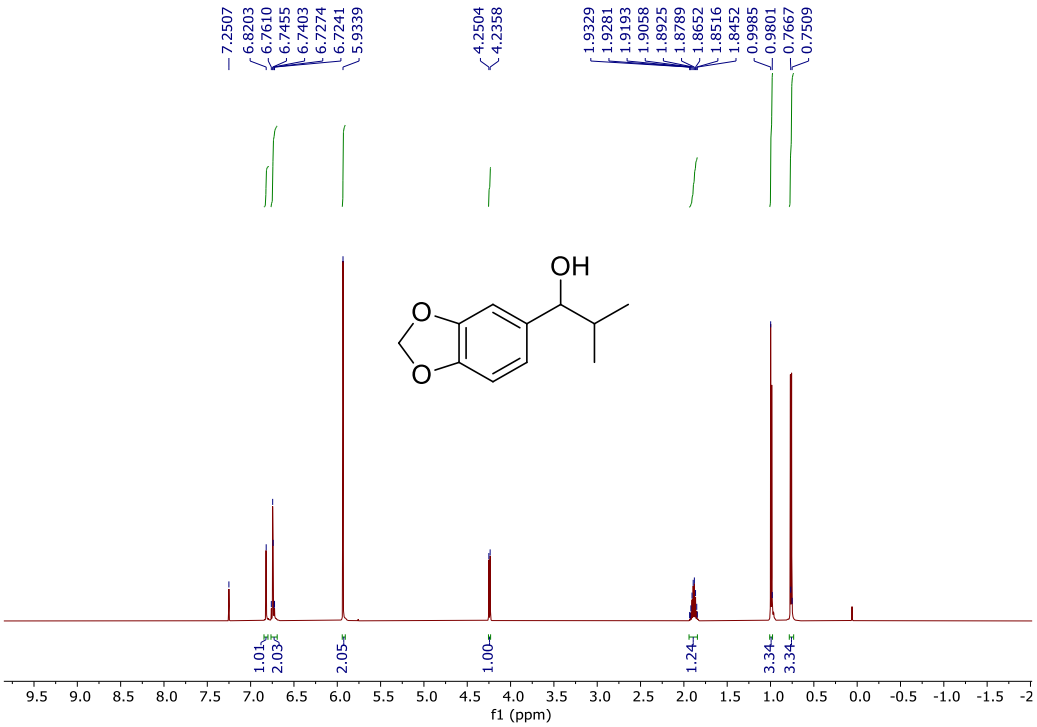

Figure S40. ^{1}H NMR Spectrum of **14** in $CDCl_3$.

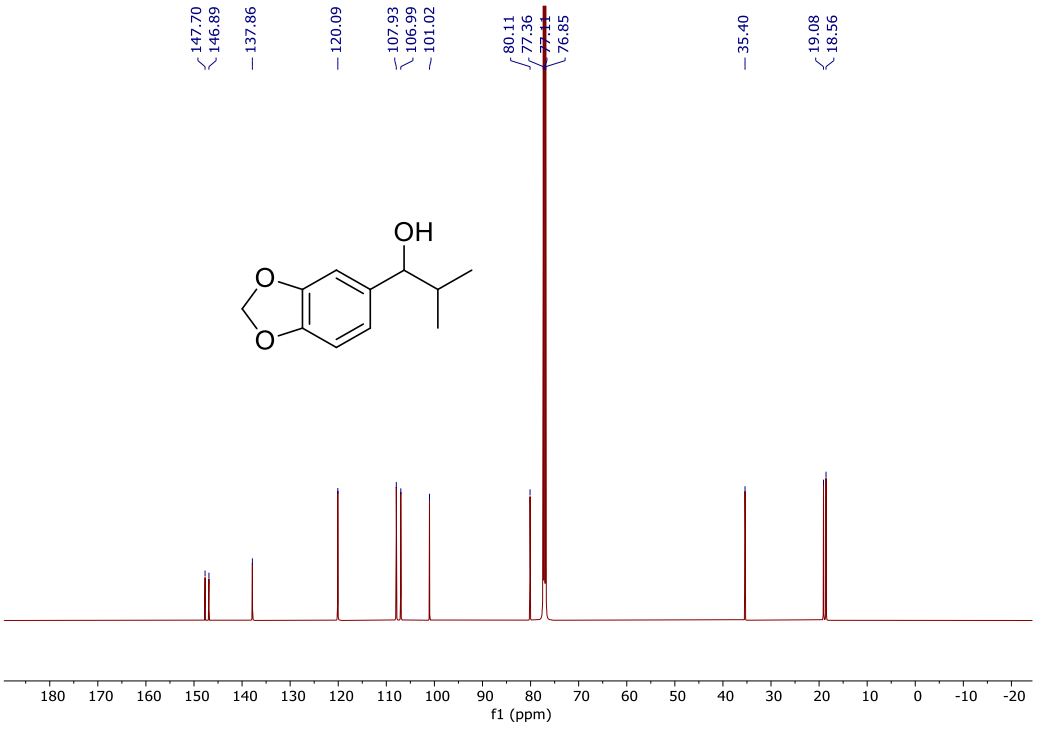

Figure S41. ^{13}C NMR Spectrum of **14** in $CDCl_3$.

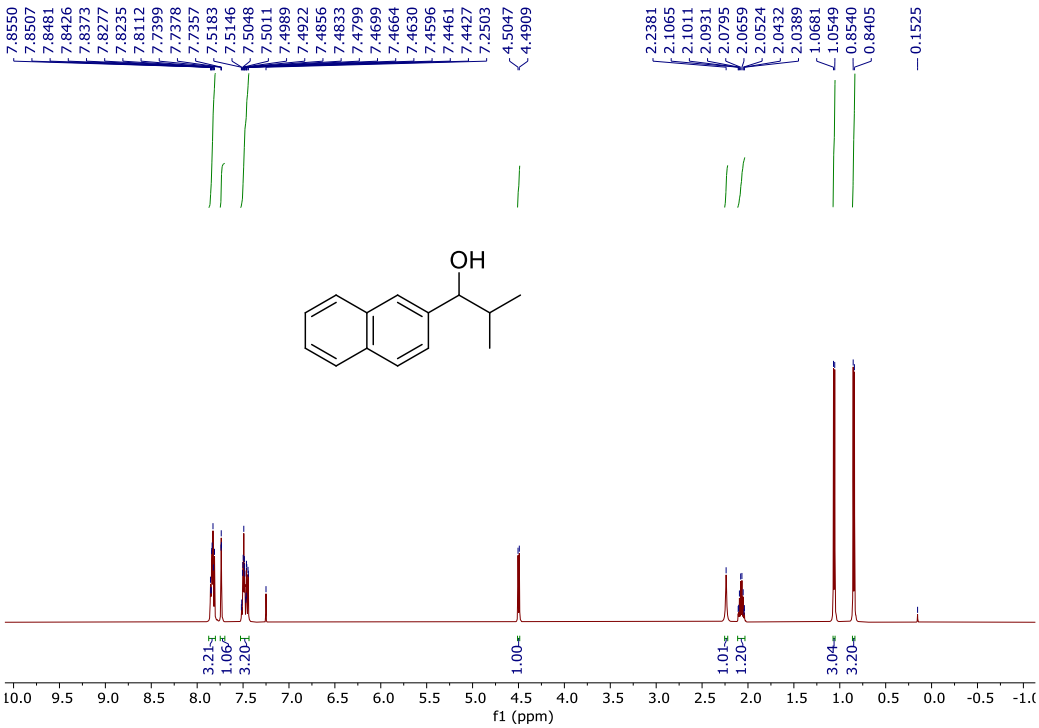

Figure S42. ^{1}H NMR Spectrum of **15** in $CDCl_3$.

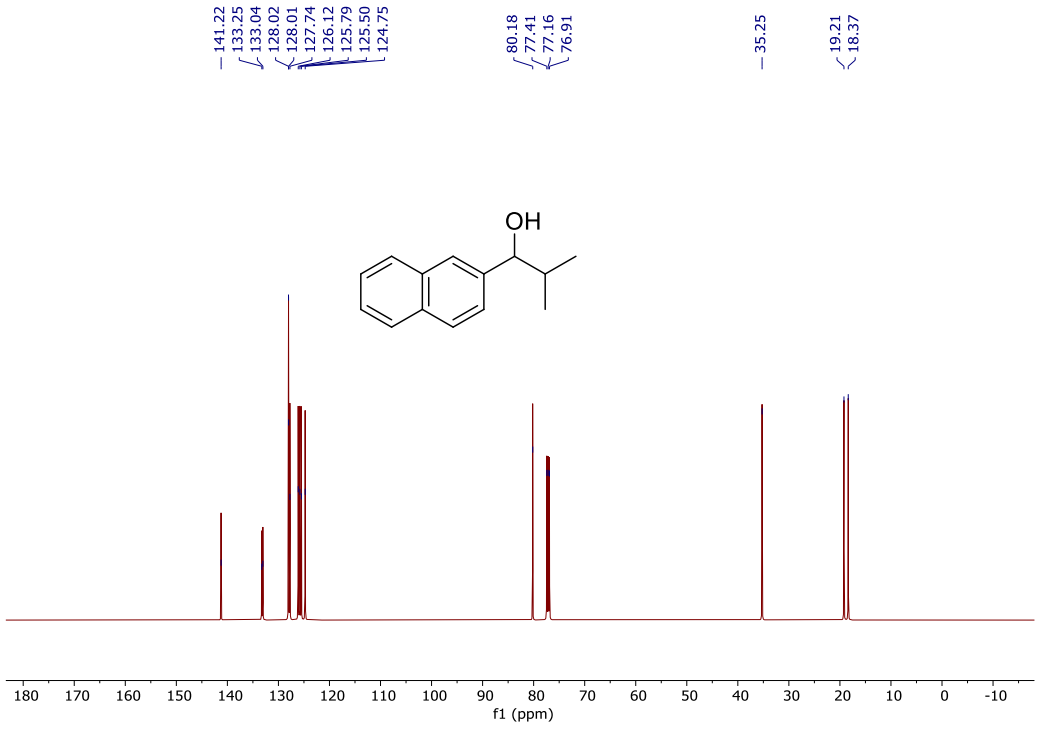

Figure S43. ^{13}C NMR Spectrum of **15** in $CDCl_3$.

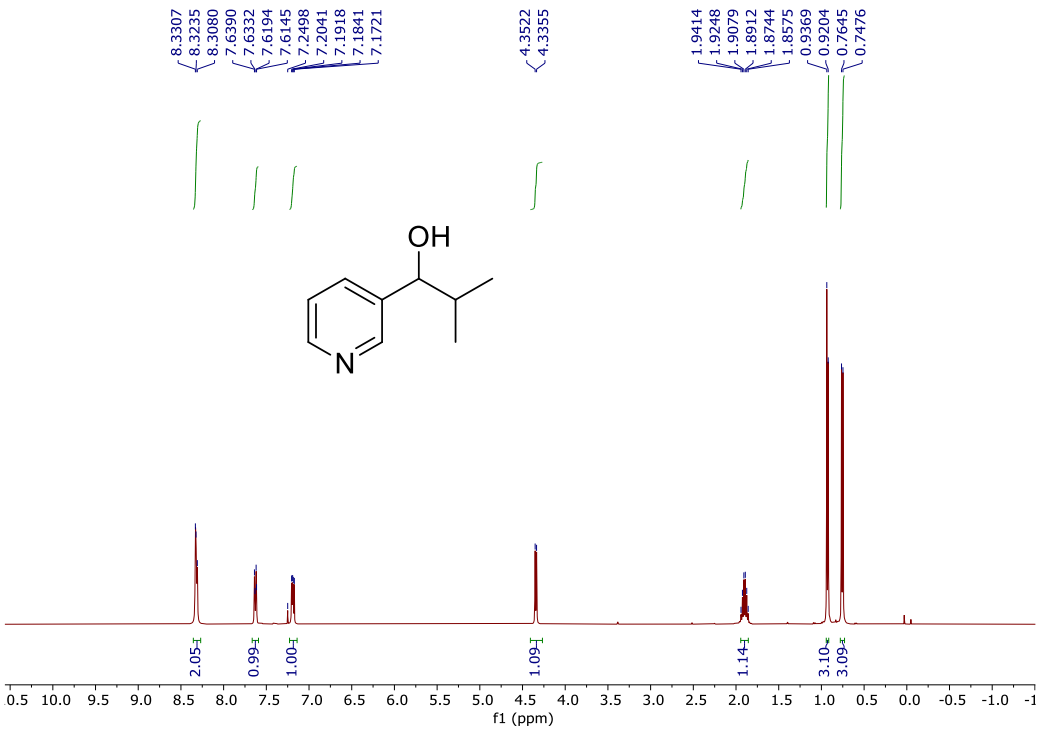

Figure S44. ^{1}H NMR Spectrum of **19** in $CDCl_3$.

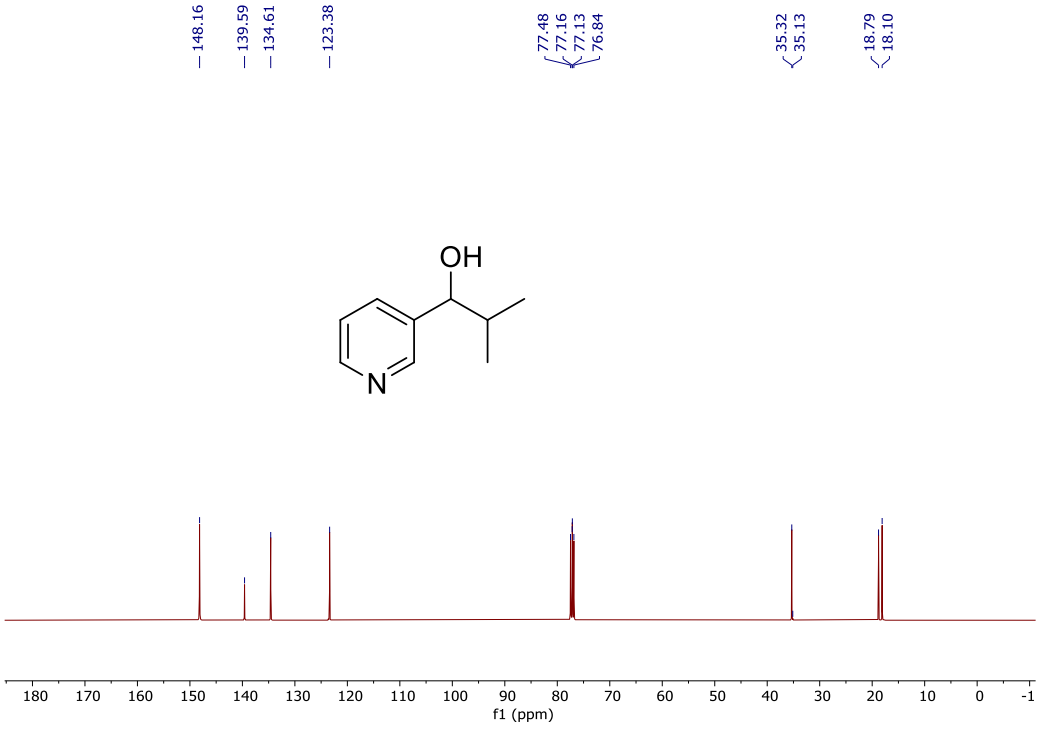

Figure S45. ^{13}C NMR Spectrum of **19** in $CDCl_3$.

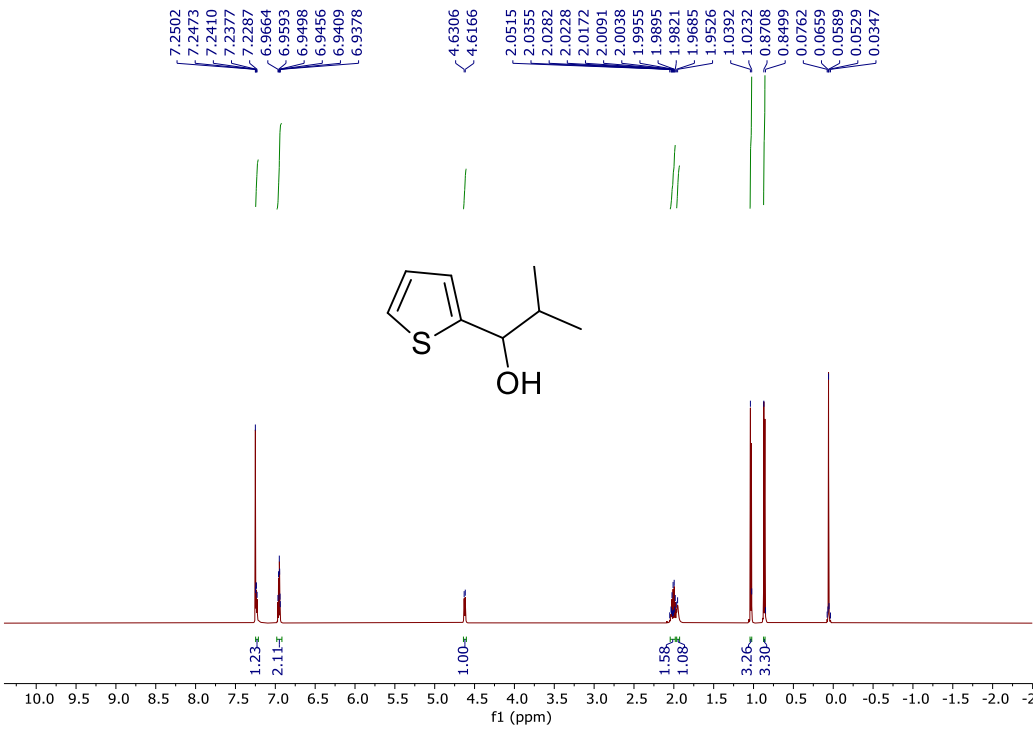

Figure S46. ^{1}H NMR Spectrum of **20** in $CDCl_3$.

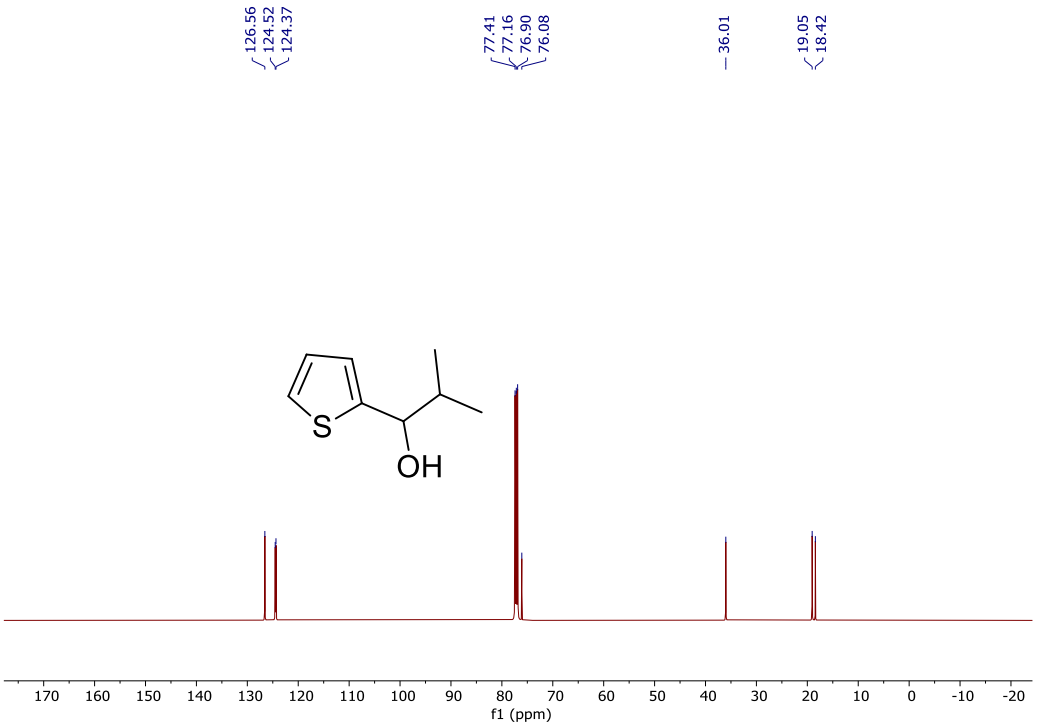

Figure S47. ^{13}C NMR Spectrum of **20** in $CDCl_3$.

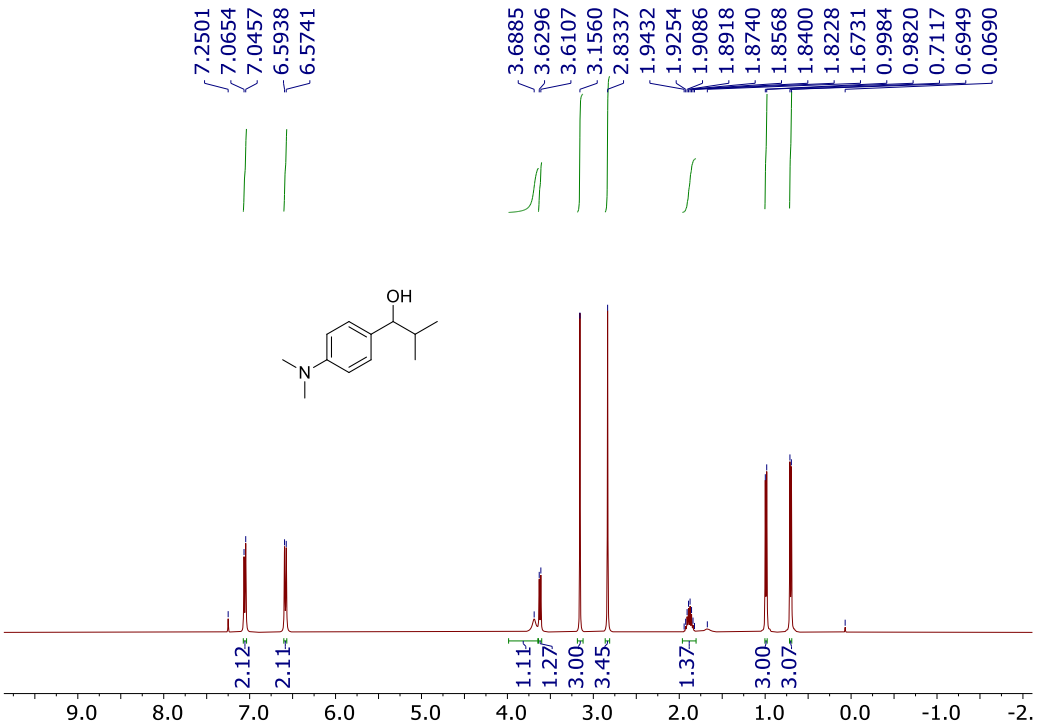

Figure S48. ^{1}H NMR Spectrum of **21** in $CDCl_3$.

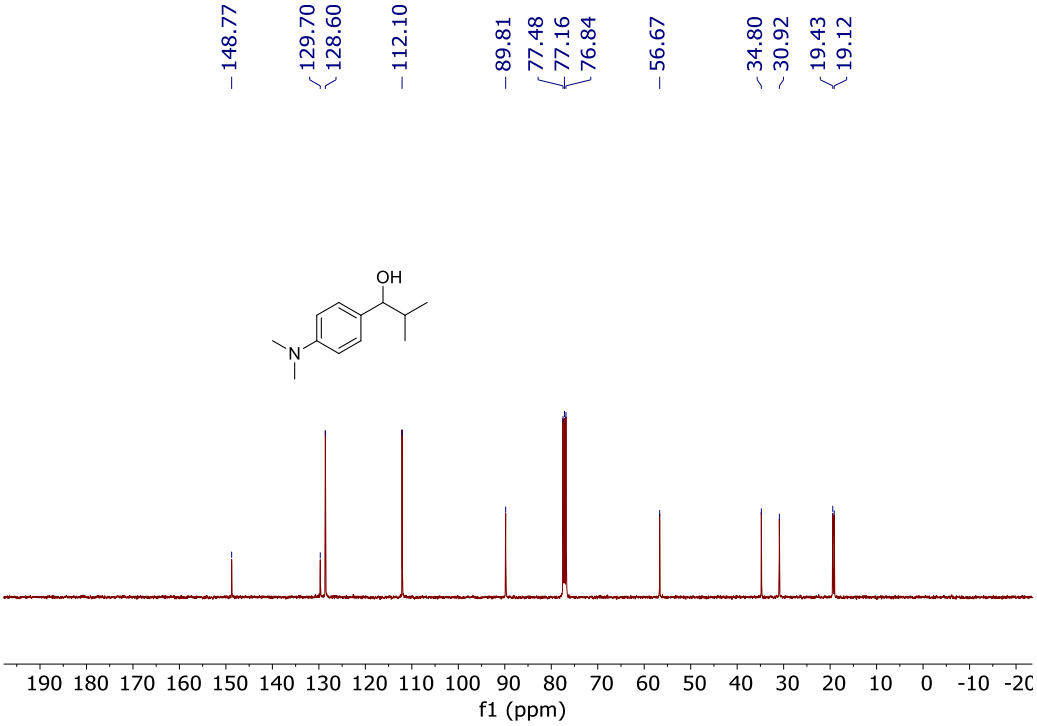

Figure S49. ^{13}C NMR Spectrum of **21** in $CDCl_3$.

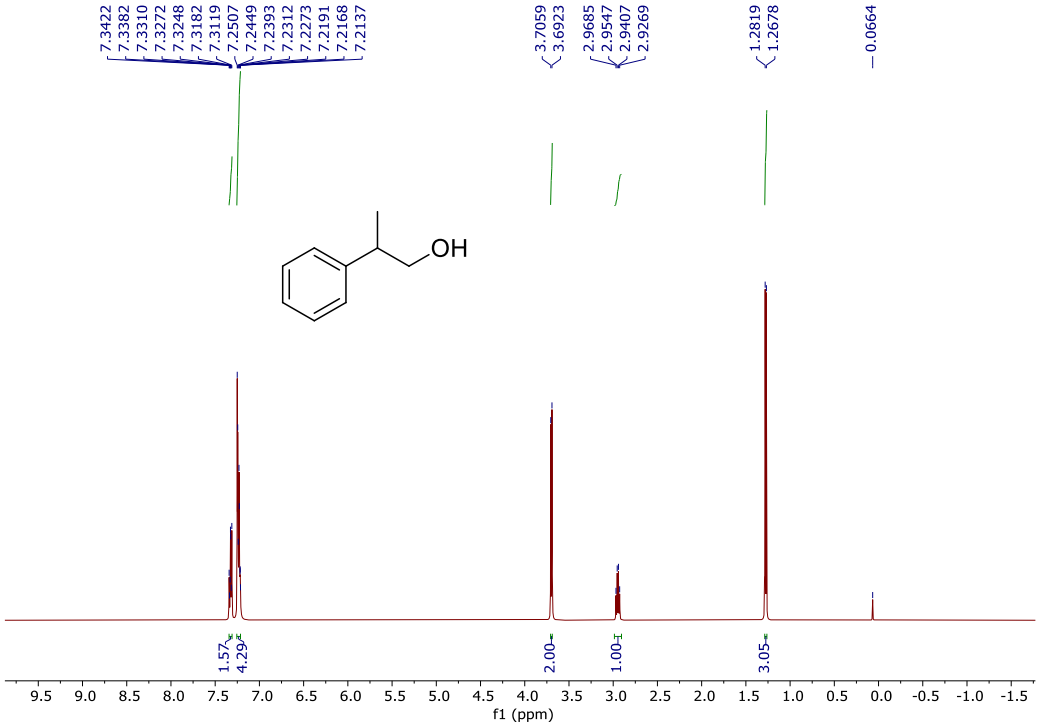

Figure S50. ^{1}H NMR Spectrum of **22** in $CDCl_3$.

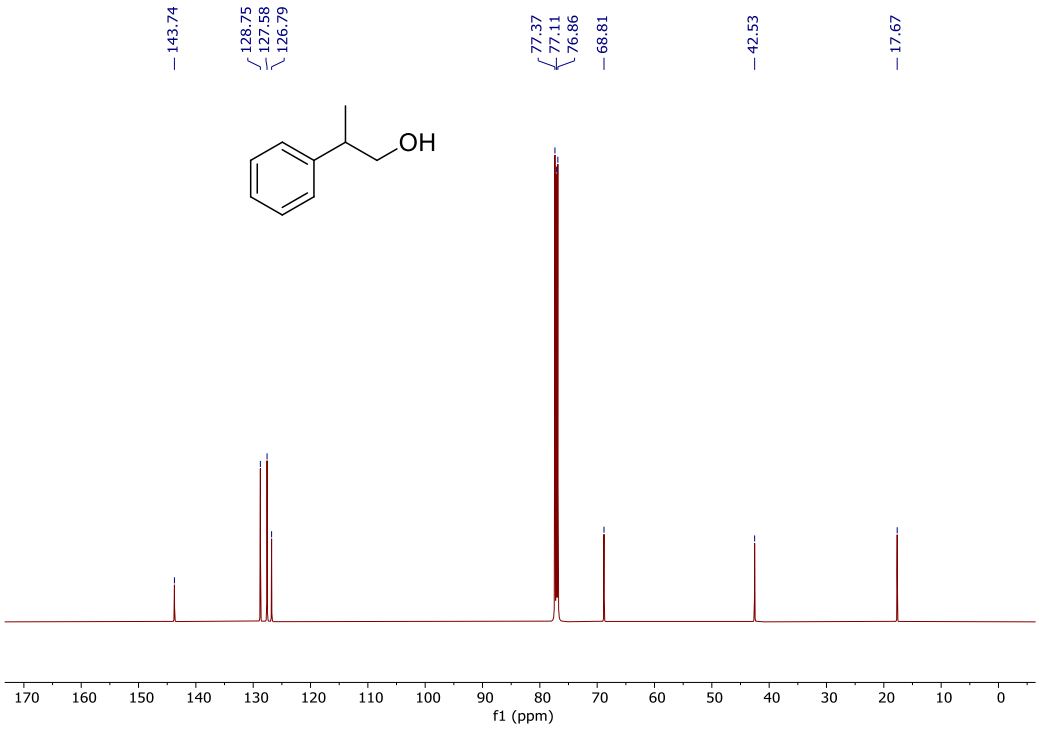

Figure S51. ^{13}C NMR Spectrum of **22** in $CDCl_3$.

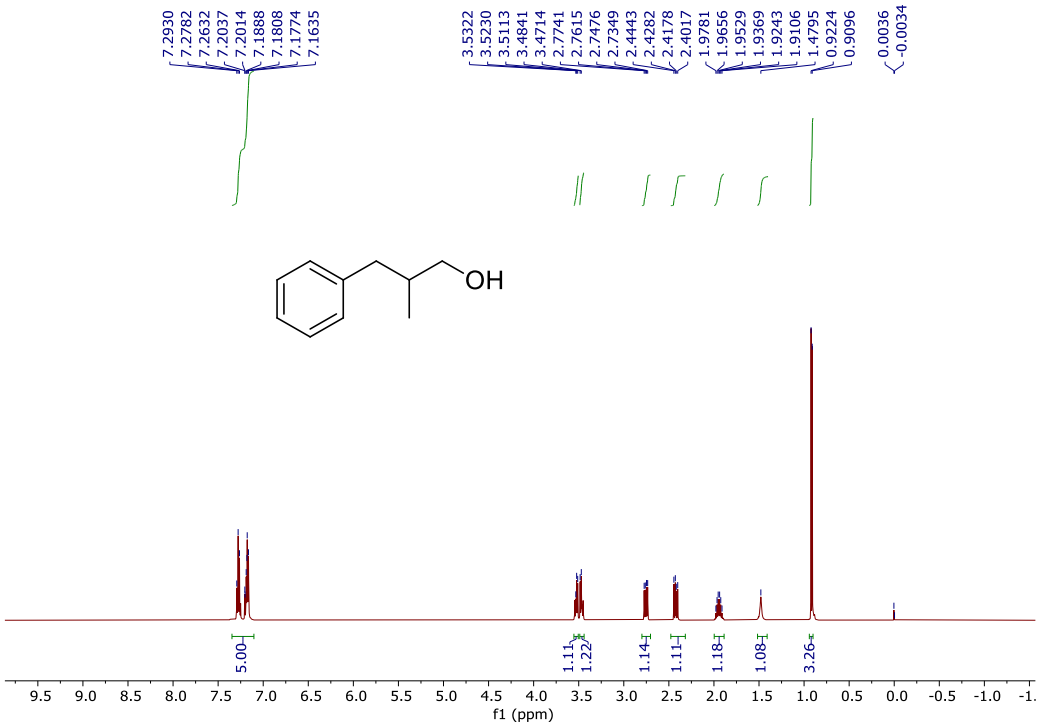

Figure S52. ^{1}H NMR Spectrum of **23** in $CDCl_3$.

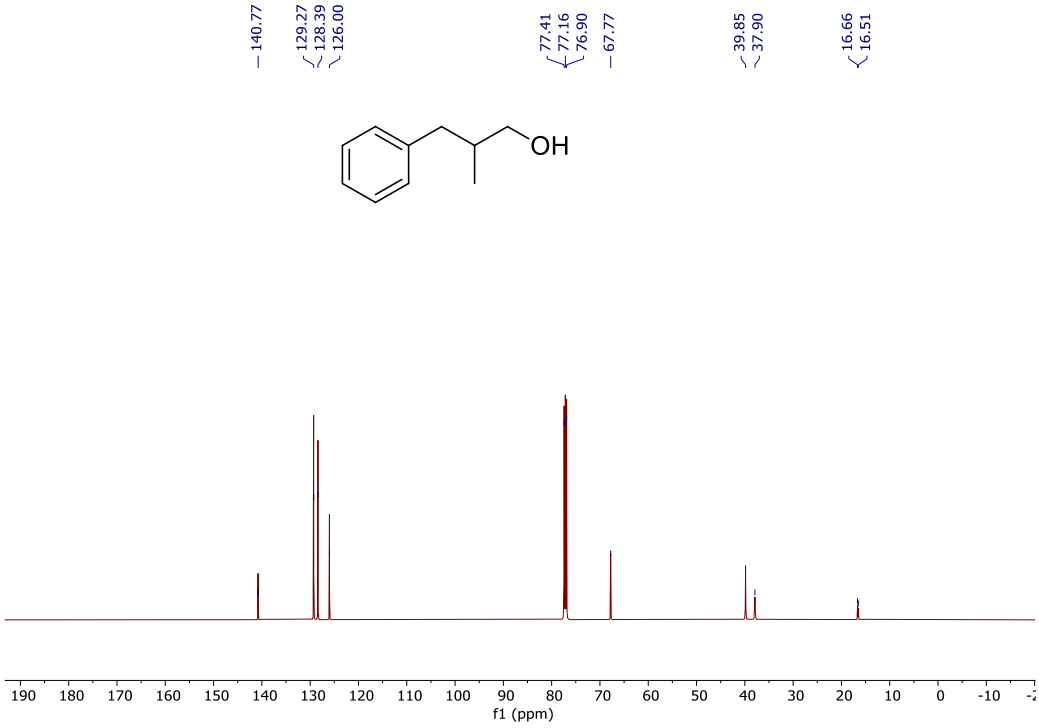

Figure S53. ^{13}C NMR Spectrum of **23** in $CDCl_3$.

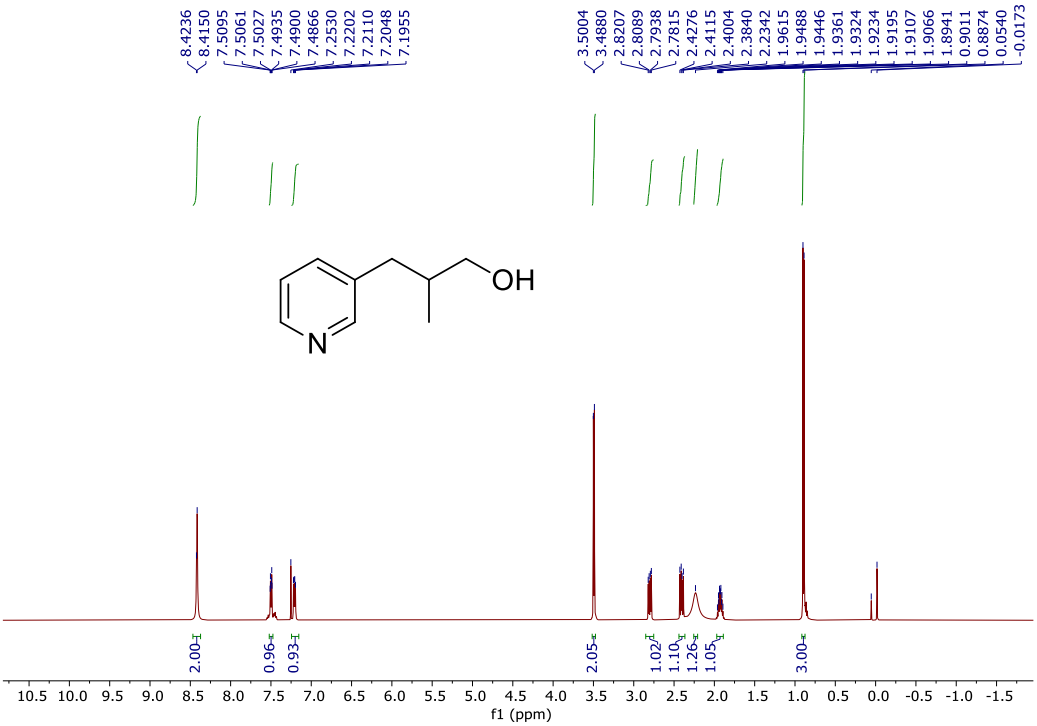

Figure S54. ^{1}H NMR Spectrum of **24** in $CDCl_3$.

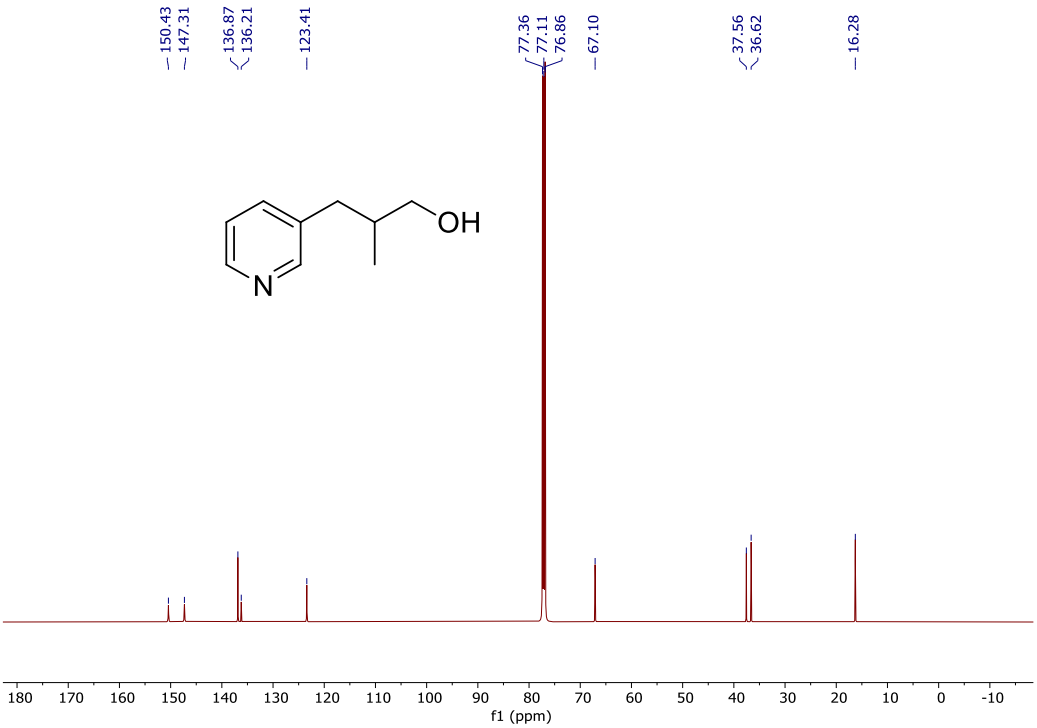

Figure S55. ^{13}C NMR Spectrum of **24** in $CDCl_3$.

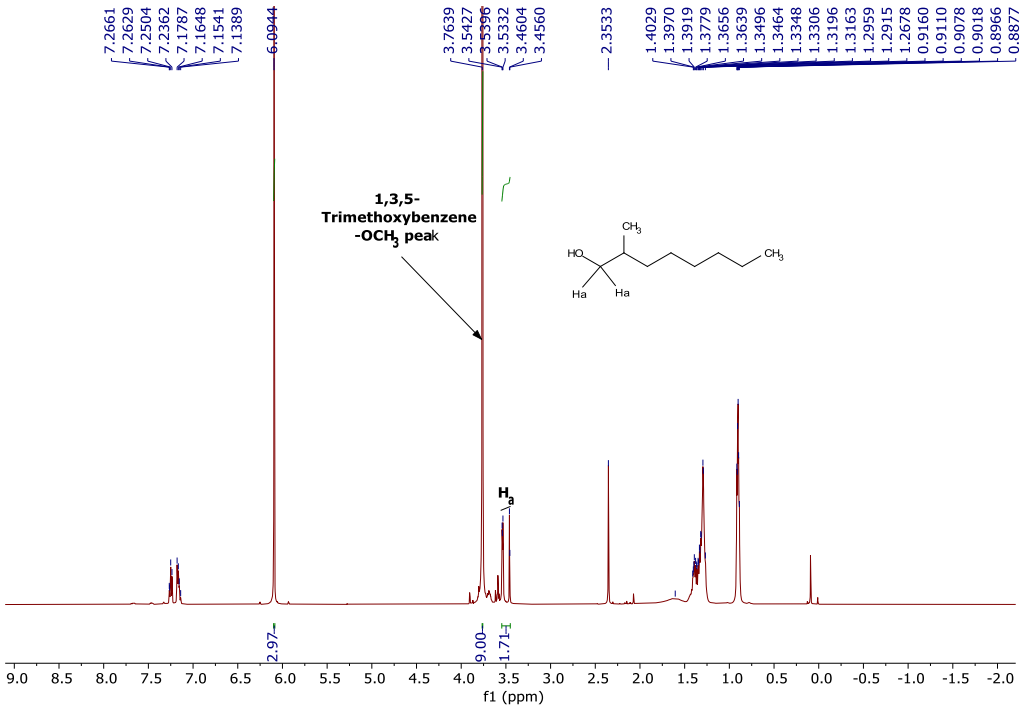

Figure S56. ^{1}H NMR Spectrum of crude reaction mixture of **25** in $CDCl_3$.

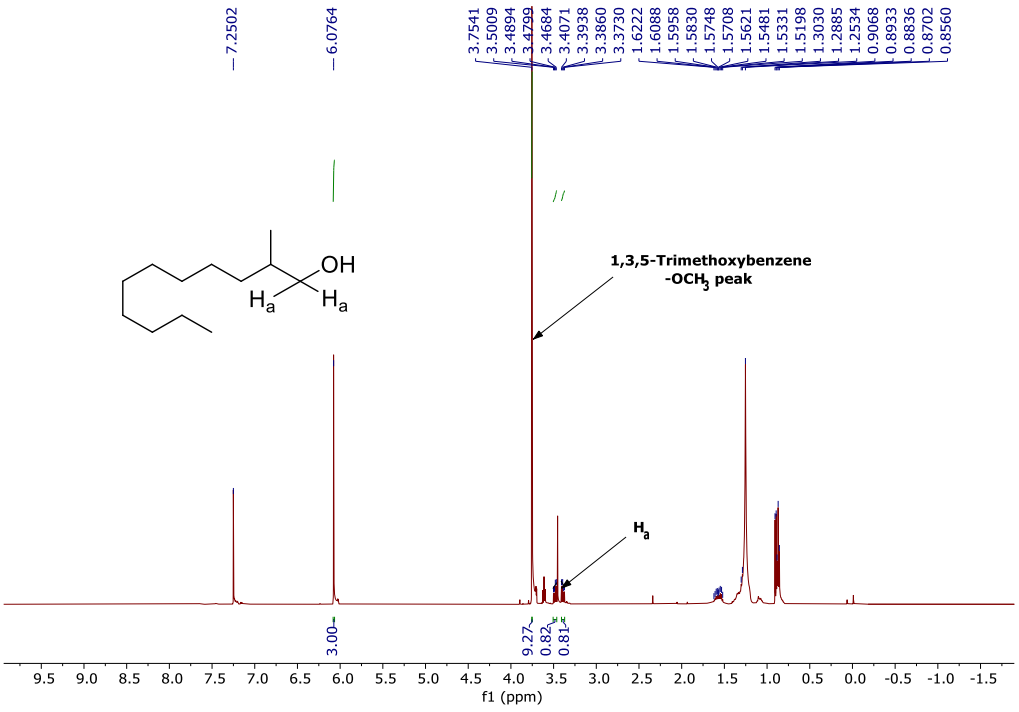

Figure S57. ^{1}H NMR Spectrum of crude reaction mixture of **26** in $CDCl_3$.

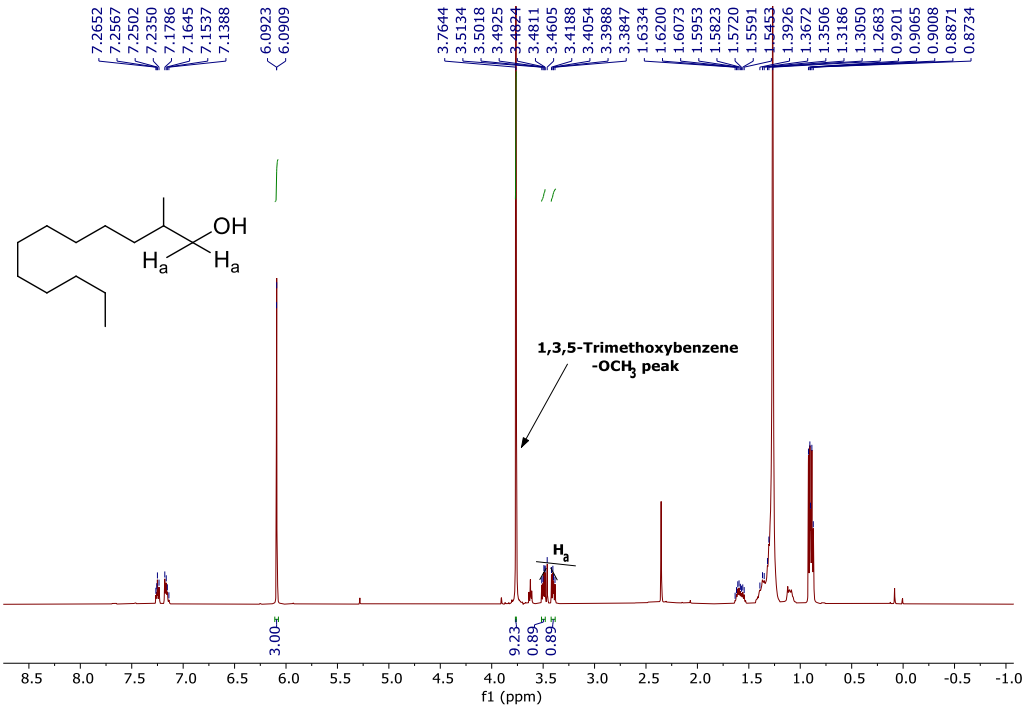

Figure S58. ^{1}H NMR Spectrum of crude reaction mixture of **27** in $CDCl_3$.

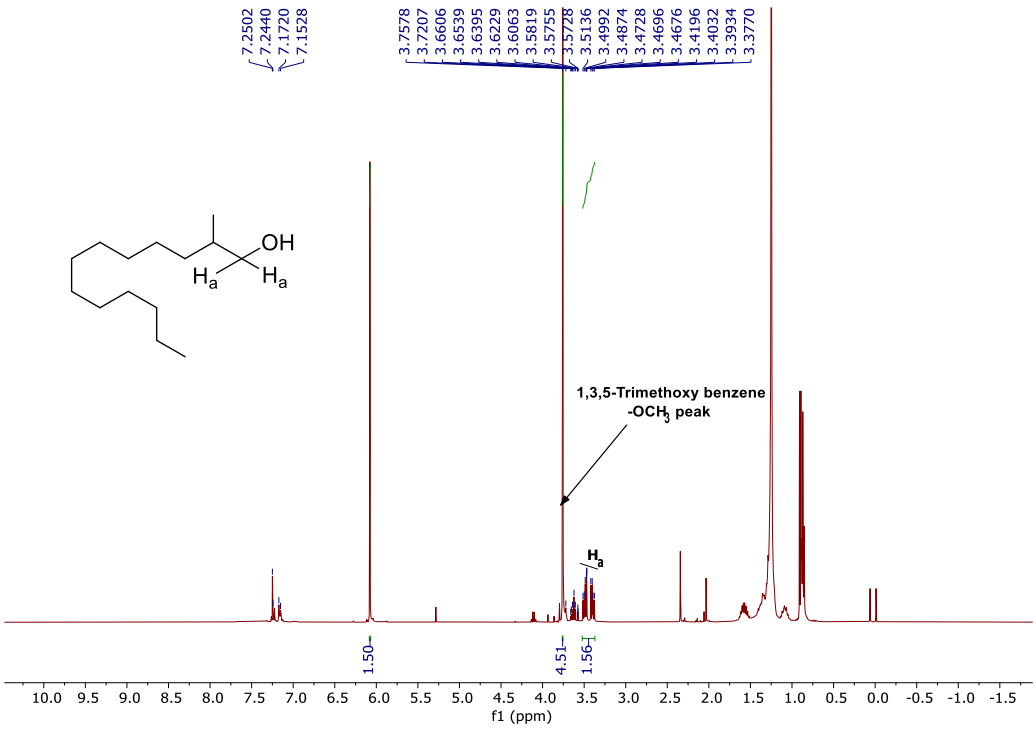

Figure S59. ^{1}H NMR Spectrum of crude reaction mixture of **28** in $CDCl_3$.

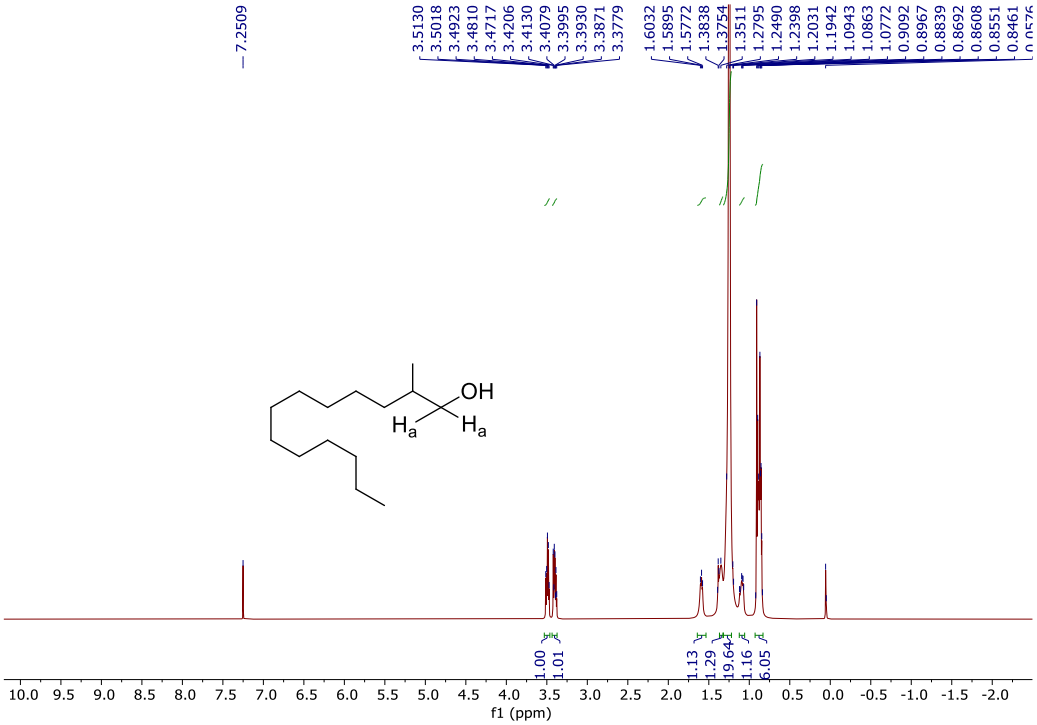

Figure S60. ^{1}H NMR Spectrum of pure **28** in $CDCl_3$.

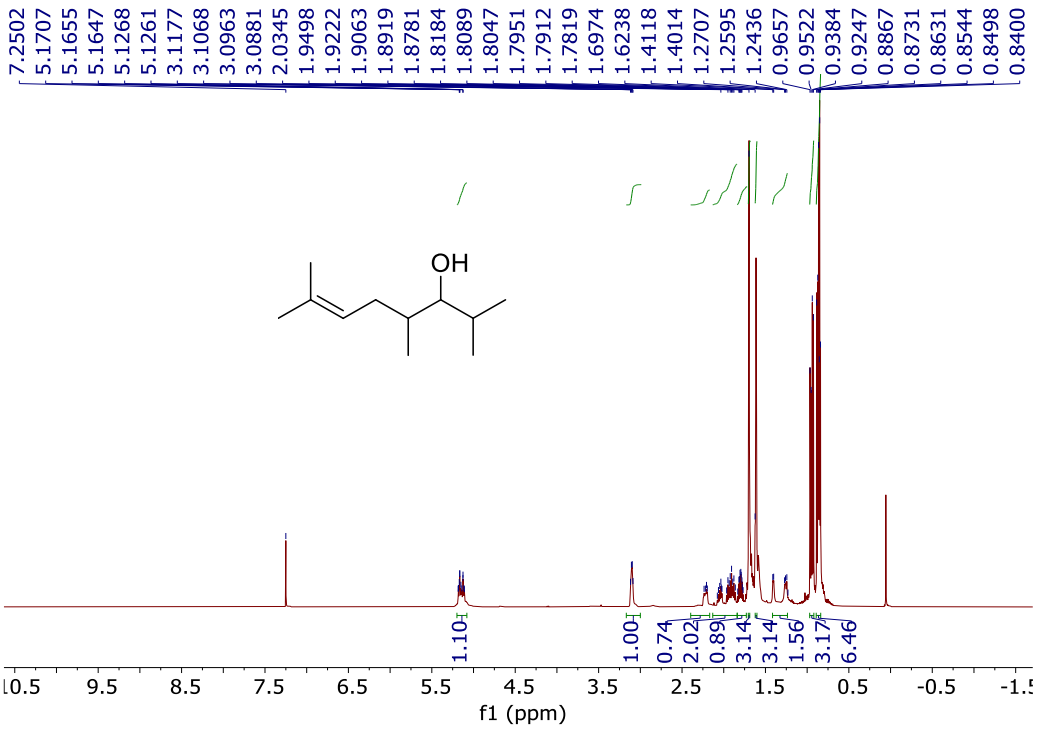

Figure S61. ^{1}H NMR Spectrum of pure **29** in $CDCl_3$.

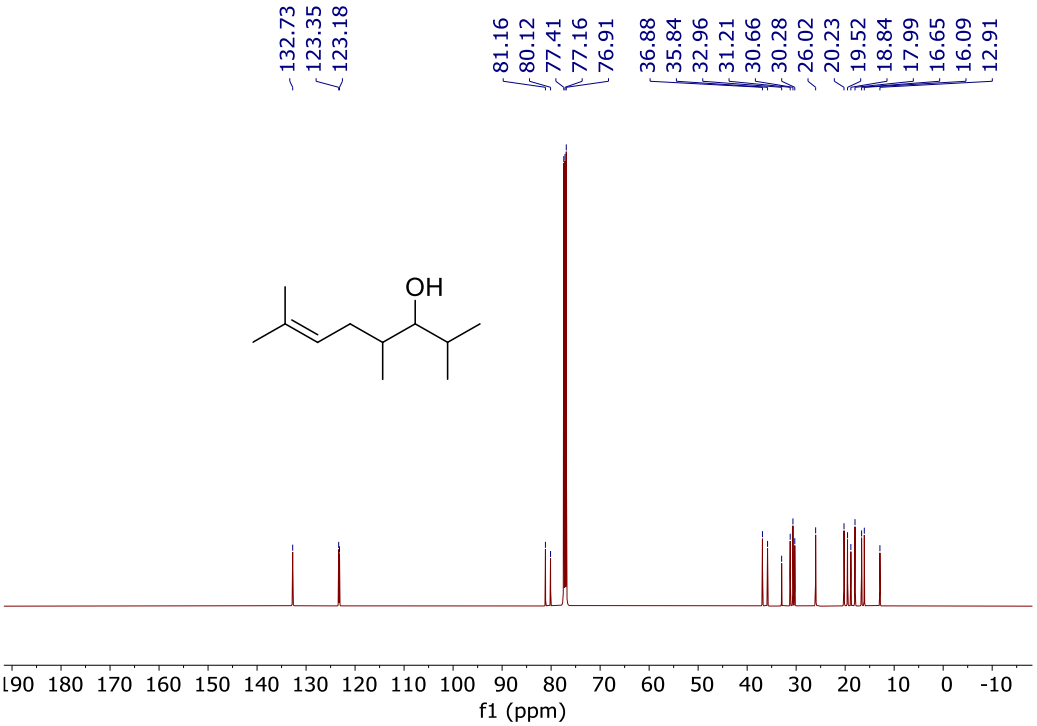

Figure S62. ^{13}C NMR Spectrum of pure **29** in $CDCl_3$.

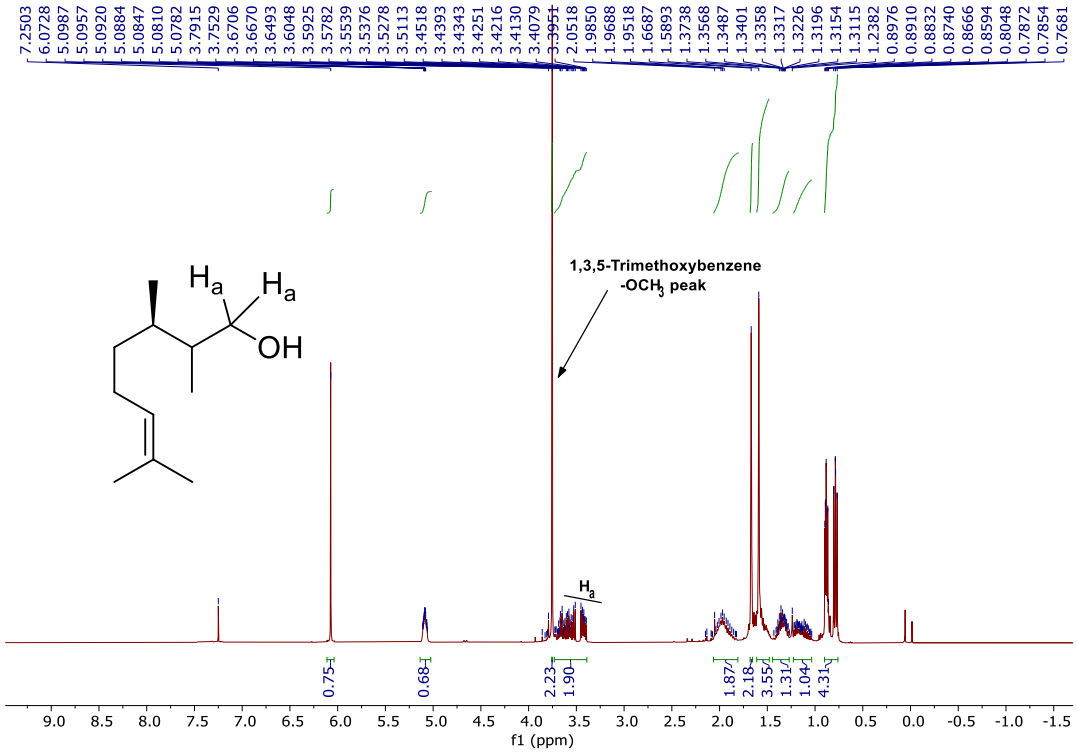

Figure S63. ^{1}H NMR Spectrum of crude reaction mixture of **30** in $CDCl_3$.

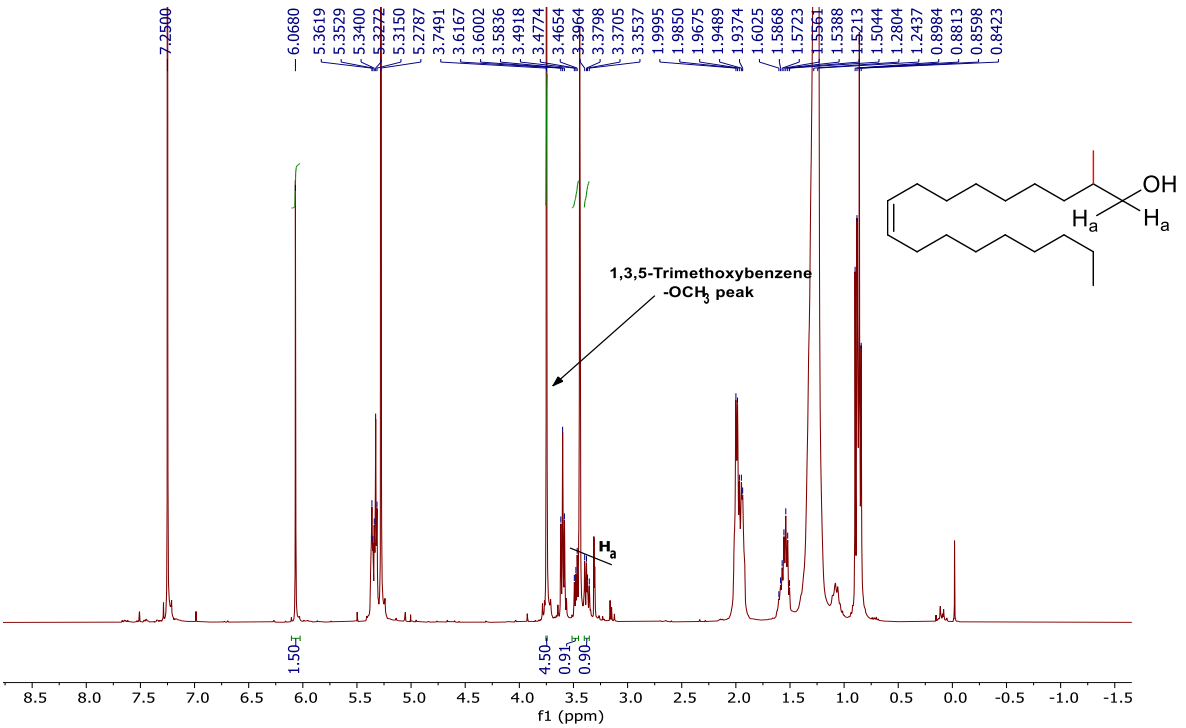

Figure S64. ^{1}H NMR Spectrum of crude reaction mixture of **31** in $CDCl_3$.

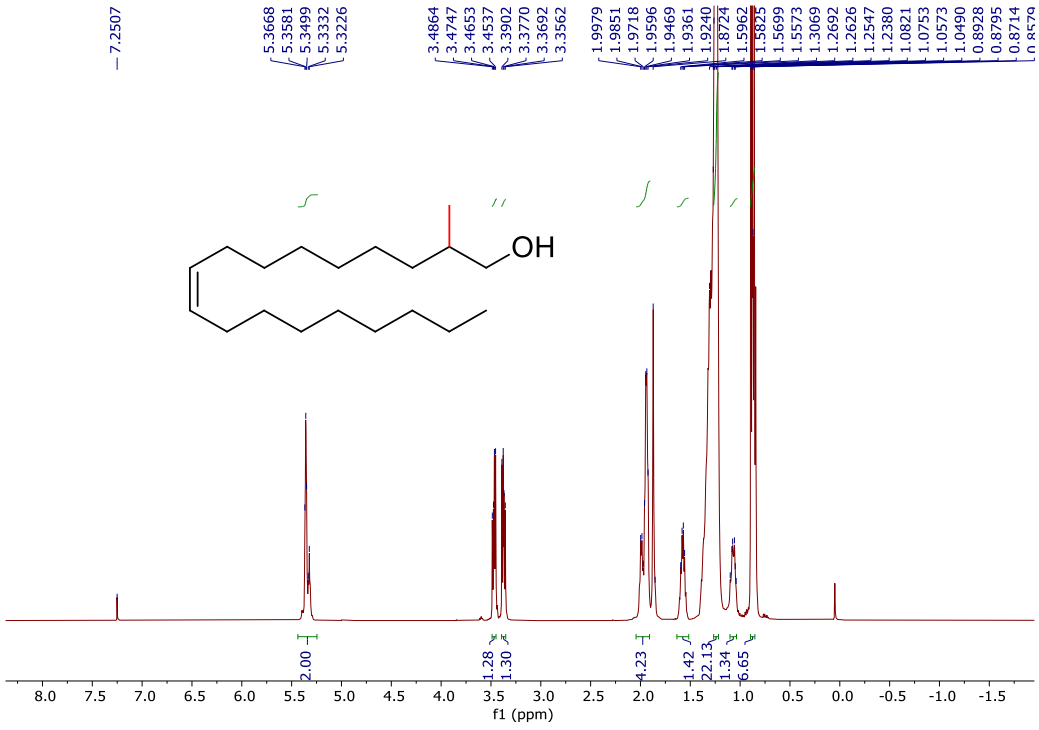

Figure S65. ^{1}H NMR Spectrum of pure **31** in $CDCl_3$.

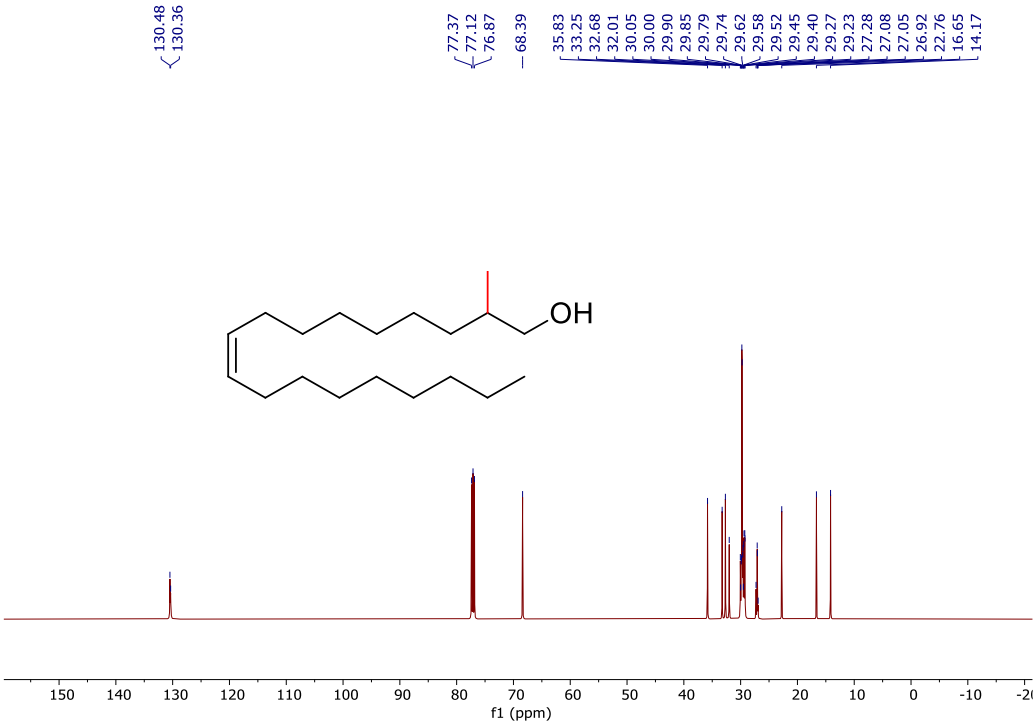

Figure S66. ^{13}C NMR Spectrum of pure **31** in $CDCl_3$.

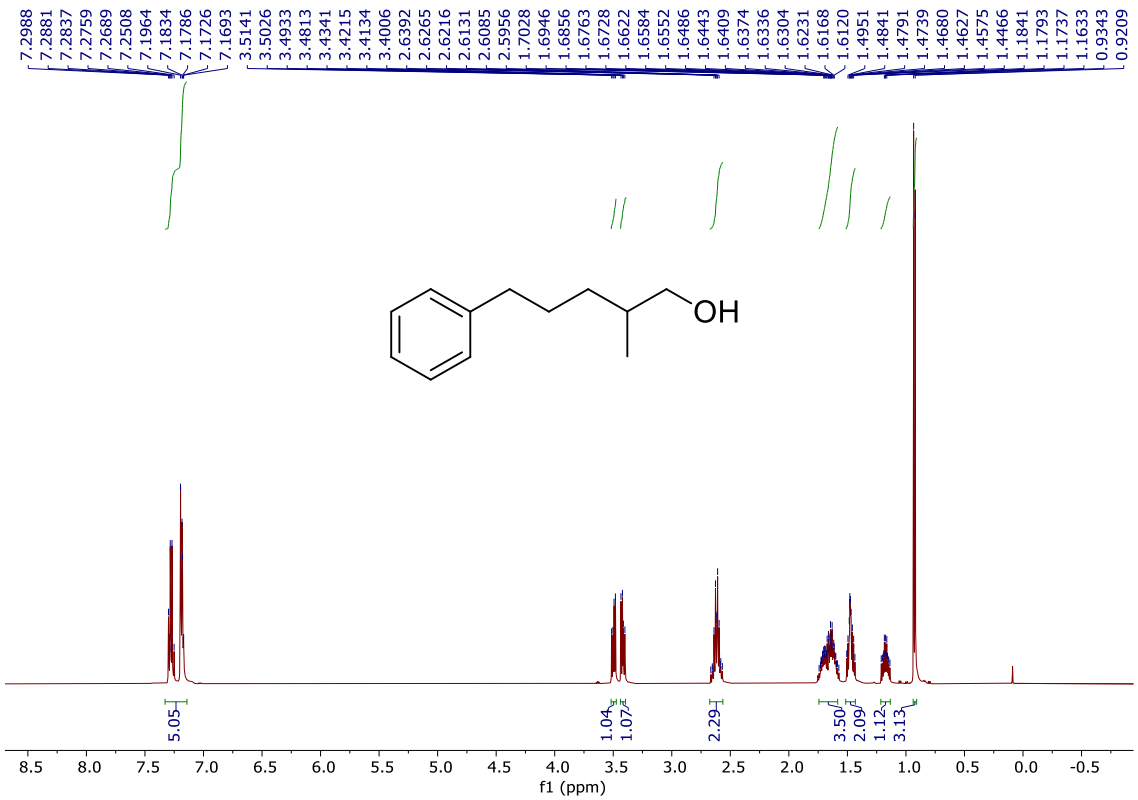

Figure S67. ^{1}H NMR Spectrum of **32** in $CDCl_3$.

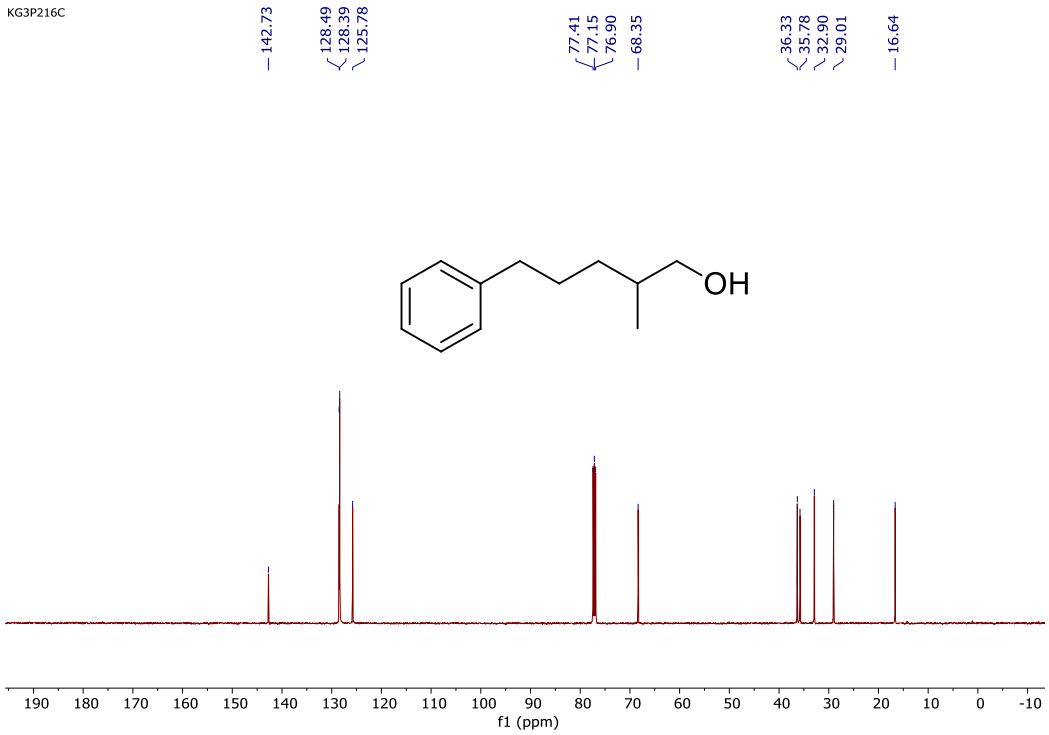

Figure S68. ^{13}C NMR Spectrum of **32** in $CDCl_3$.